To cite this version :

Le Roch, Alexandre and Goiffon, Vincent and Durnez, Clémentine and Magnan, Pierre and Virmontois, Cédric and Pistre, L. and Belloir, Jean-Marc Radiation-Induced Defects in a Commercial Image Sensor for Space Applications. (2017) In: CNES Workshop: CMOS Image Sensors for High Performance Applications, 21 November 2017 - 22 November 2017 (Toulouse, France).

CENTRE NATIONAL D'ÉTUDES SPATIALES

Institut Supérieur de l'Aéronautique et de l'Espace
SUPAERO

Radiation Induced Defects in Commercial Image Sensor for Space Applications

A. Le Roch, V. Goiffon, C. Durnez, P. Magnan
Université de Toulouse, ISAE SUPAERO, 31055 Toulouse, France.

C. Virmontois, L. Pistre, J-M. Belloir
Centre National d'Etudes Spatiales (CNES), 31400 Toulouse, France.

Context and Goal

- CMOS Image Sensor (CIS) are considered as the perennial path for future space imaging and especially the PPD technology.

Context and Goal

- CMOS Image Sensor (CIS) are considered as the perennial path for future space imaging and especially the PPD technology.
- Particles from space are likely to generate Displacement Damage Dose (DDD).

Context and Goal

- CMOS Image Sensor (CIS) are considered as the perennial path for future space imaging and especially the PPD technology.
- Particles from space are likely to generate Displacement Damage Dose (DDD).

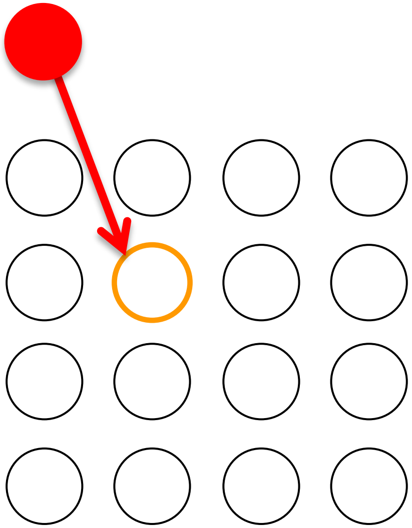

Context and Goal

- CMOS Image Sensor (CIS) are considered as the perennial path for future space imaging and especially the PPD technology.

- Particles from space are likely to generate Displacement Damage Dose (DDD).

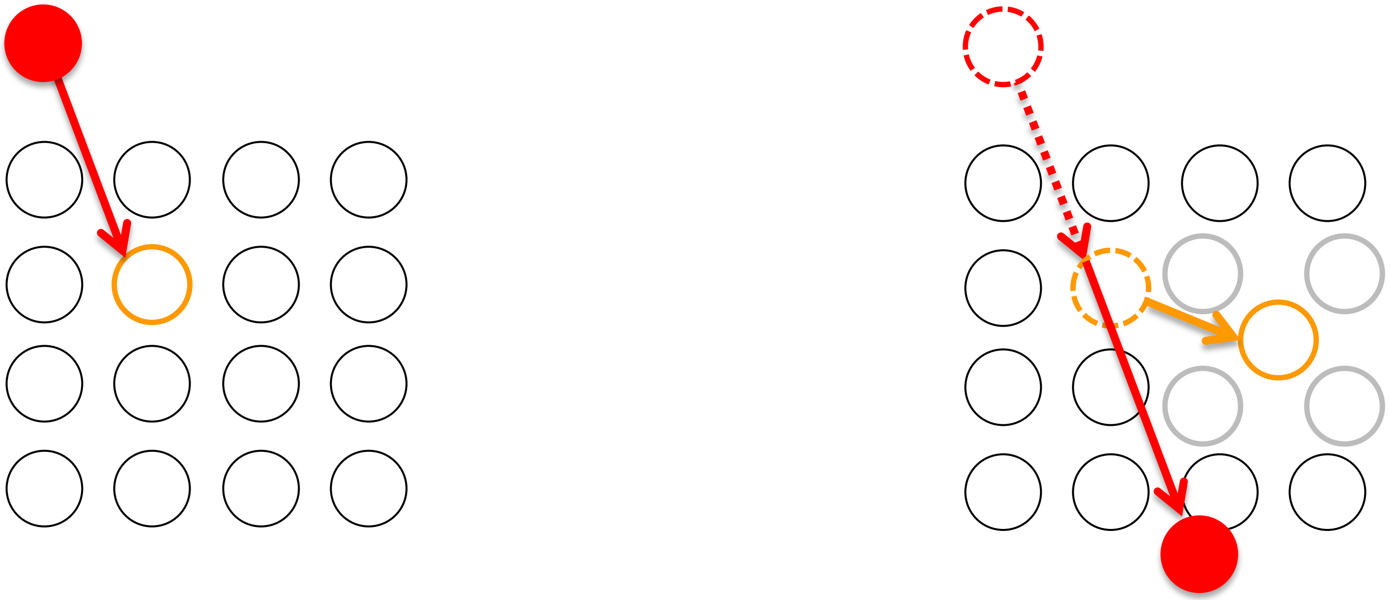

Context and Goal

A. JAY and al. (NSREC 2016)

Context and Goal

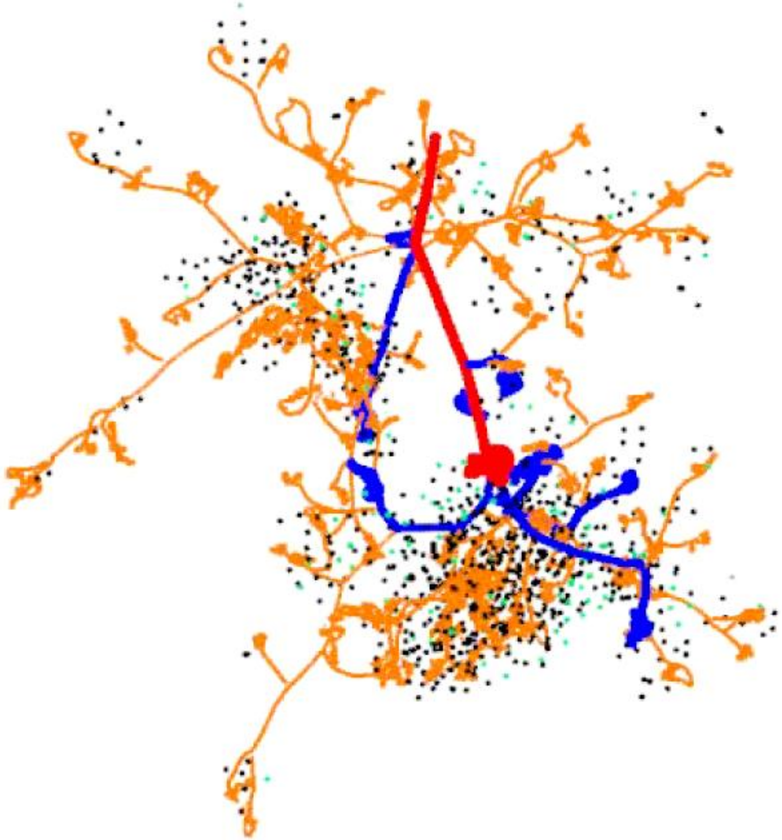

A. JAY and al. (NSREC 2016)

- Displaced Si atoms create stable defects. Such defects act as generation centers and lead to a dark current increase.

Context and Goal

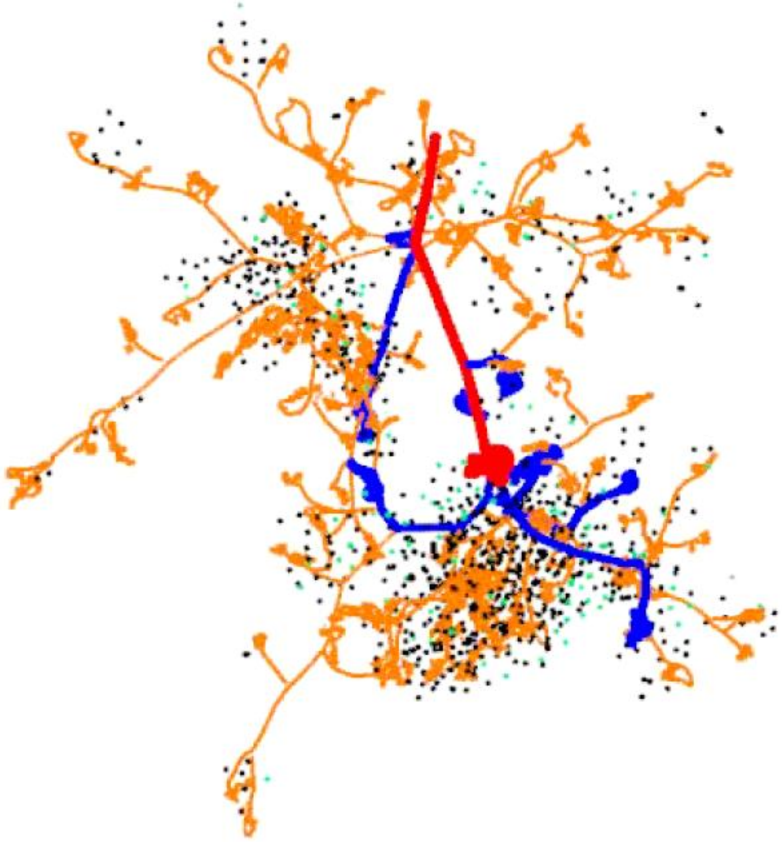

A. JAY and al. (NSREC 2016)

- Displaced Si atoms create stable defects. Such defects act as generation centers and lead to a dark current increase.
- Defects creation mechanisms and annealing behaviors are needed for a better understanding of radiation induced dark current increase.

Context and Goal

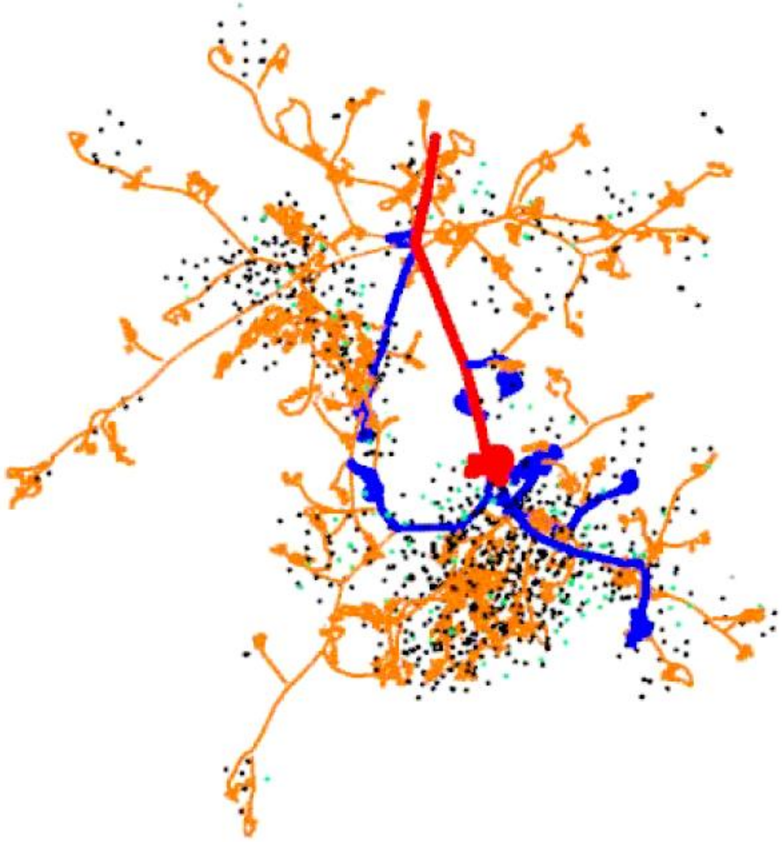

A. JAY and al. (NSREC 2016)

- Displaced Si atoms create stable defects. Such defects act as generation centers and lead to a dark current increase.
- Defects creation mechanisms and annealing behaviors are needed for a better understanding of radiation induced dark current increase.
- The main goal is to find a mitigation technique.

Dark Current Spectroscopy (DCS)

- DCS is used to charaterize radiation induced defects throughout the dark current distribution of all the pixels of the matrix.

Dark Current Spectroscopy (DCS)

- DCS is used to charaterize radiation induced defects throughout the dark current distribution of all the pixels of the matrix.
- The per pixel dark current relies on silicon sampled by the PPD depleted volume.

Dark Current Spectroscopy (DCS)

- DCS is used to charaterize radiation induced defects throughout the dark current distribution of all the pixels of the matrix.
- The per pixel dark current relies on silicon sampled by the PPD depleted volume.

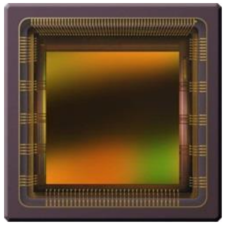

Dark Current Spectroscopy (DCS)

- DCS is used to charaterize radiation induced defects throughout the dark current distribution of all the pixels of the matrix.
- The per pixel dark current relies on silicon sampled by the PPD depleted volume.

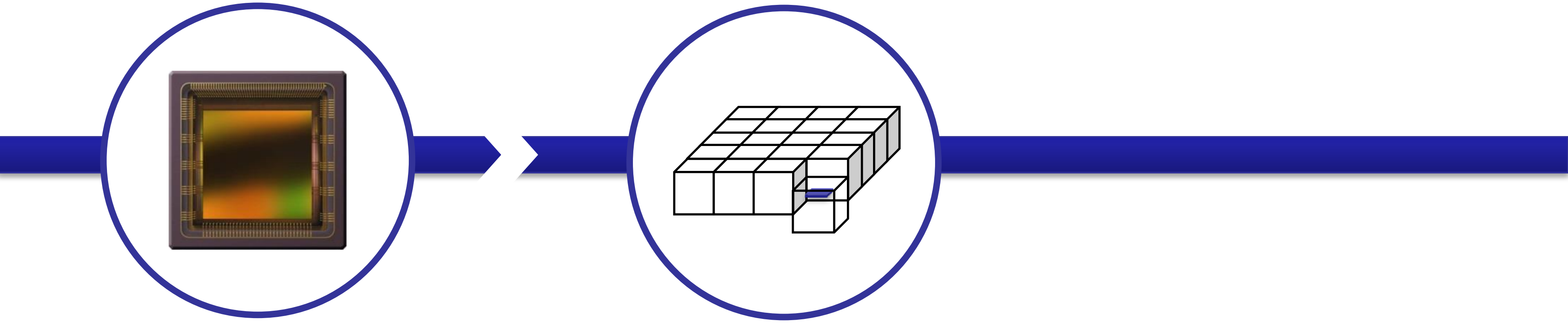

Dark Current Spectroscopy (DCS)

- DCS is used to charaterize radiation induced defects throughout the dark current distribution of all the pixels of the matrix.
- The per pixel dark current relies on silicon sampled by the PPD depleted volume.

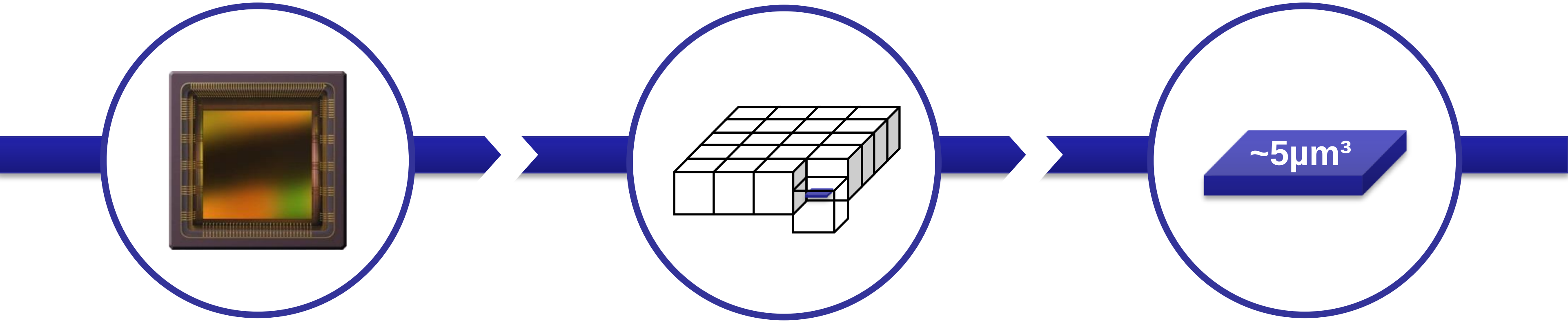

Dark Current Spectroscopy (DCS)

- DCS is used to charaterize radiation induced defects throughout the dark current distribution of all the pixels of the matrix.
- The per pixel dark current relies on silicon sampled by the PPD depleted volume.

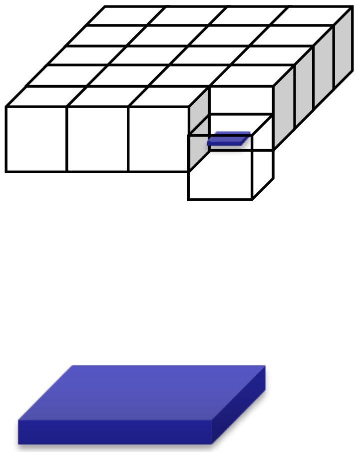

Dark Current Spectroscopy (DCS)

- DCS is used to charaterize radiation induced defects throughout the dark current distribution of all the pixels of the matrix.
- The per pixel dark current relies on silicon sampled by the PPD depleted volume.

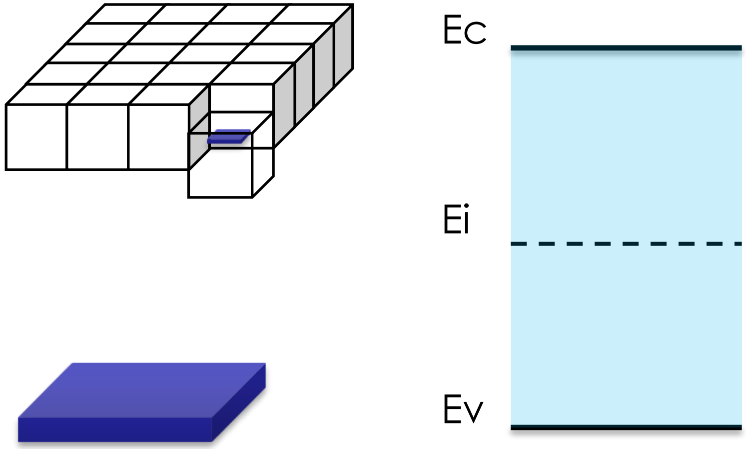

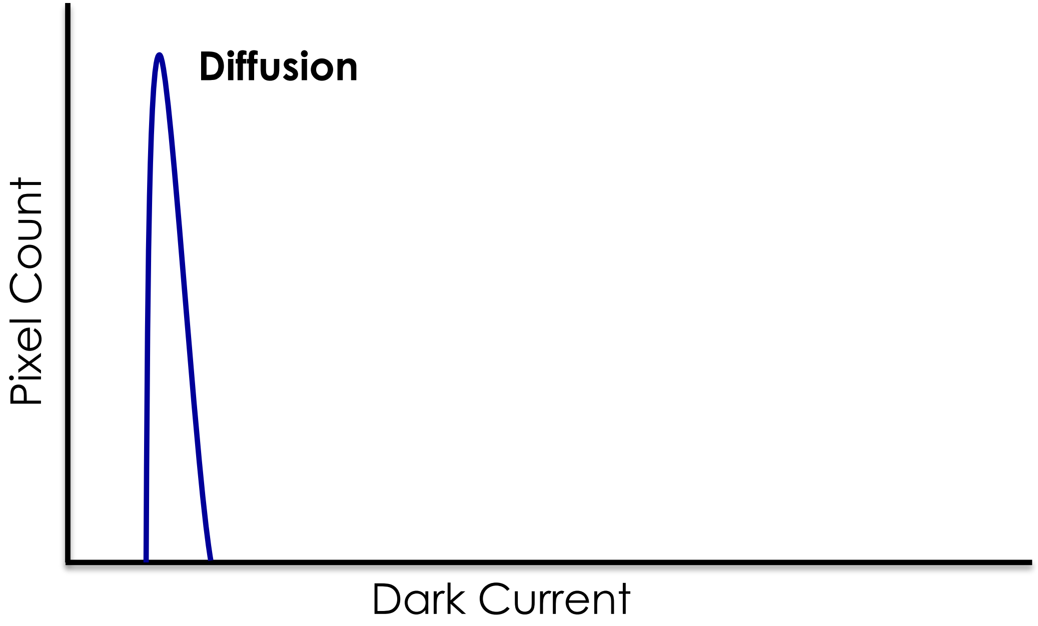

Dark Current Spectroscopy (DCS)

- DCS is used to charaterize radiation induced defects throughout the dark current distribution of all the pixels of the matrix.
- The per pixel dark current relies on silicon sampled by the PPD depleted volume.

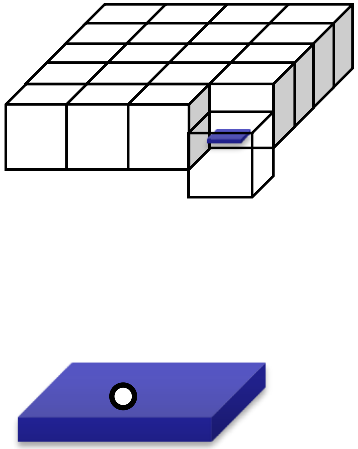

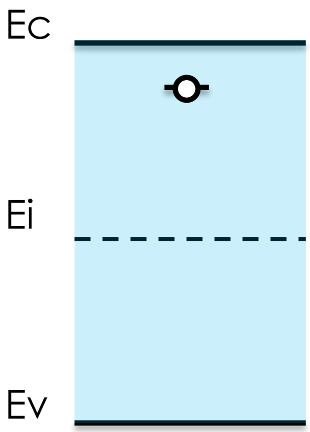

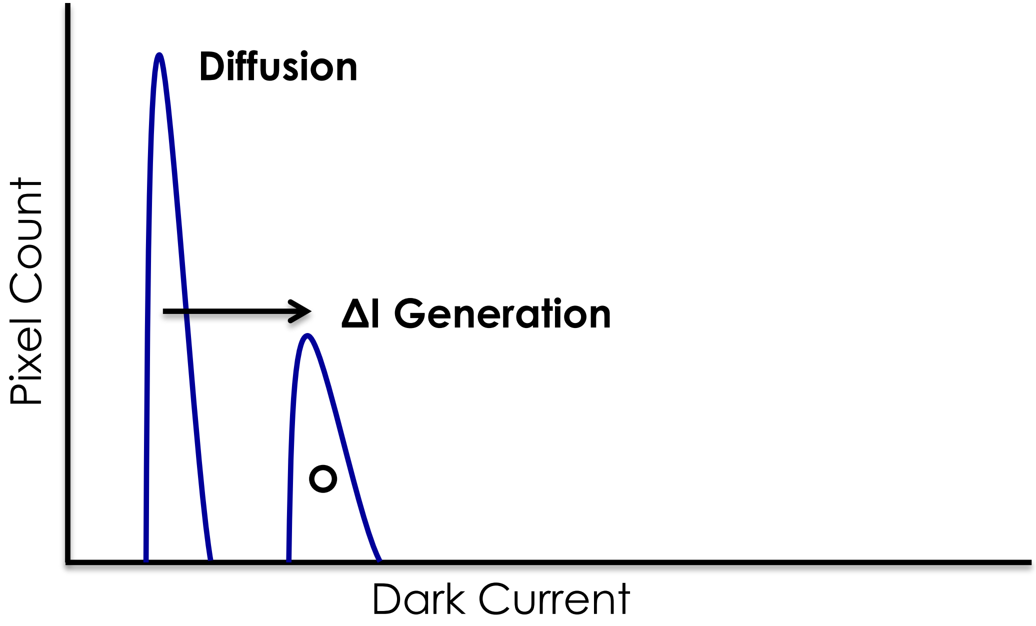

Dark Current Spectroscopy (DCS)

- DCS is used to charaterize radiation induced defects throughout the dark current distribution of all the pixels of the matrix.
- The per pixel dark current relies on silicon sampled by the PPD depleted volume.

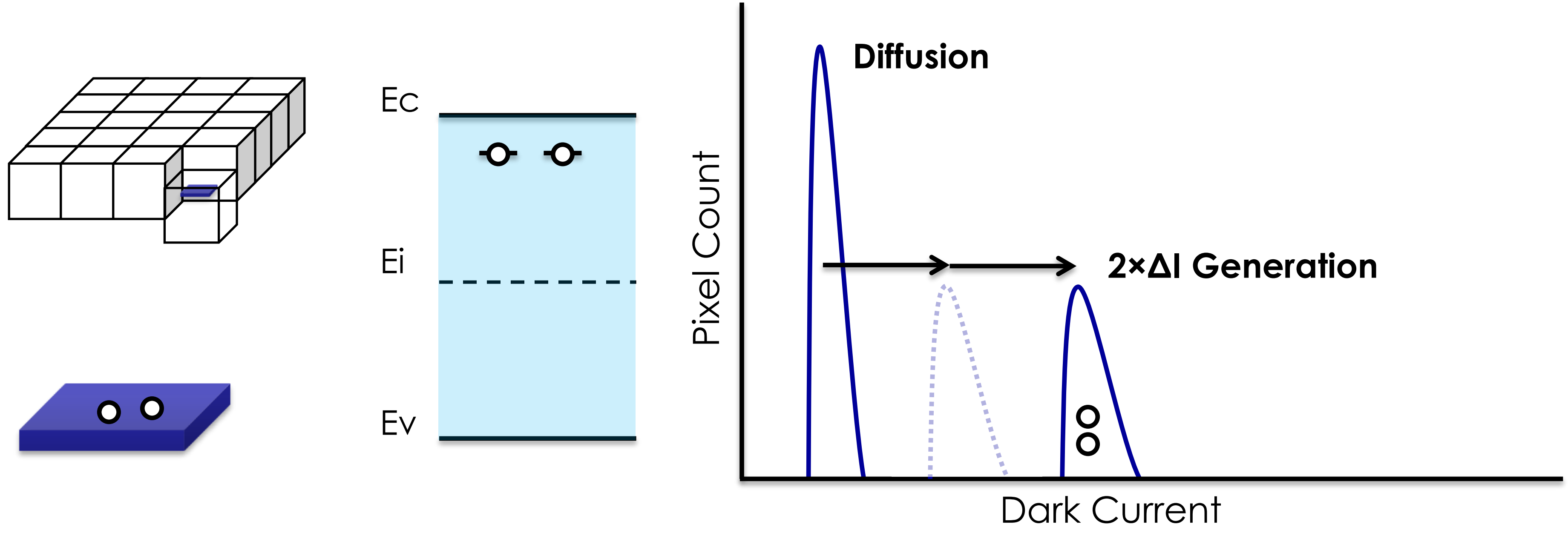

Dark Current Spectroscopy (DCS)

- DCS is used to charaterize radiation induced defects throughout the dark current distribution of all the pixels of the matrix.
- The per pixel dark current relies on silicon sampled by the PPD depleted volume.

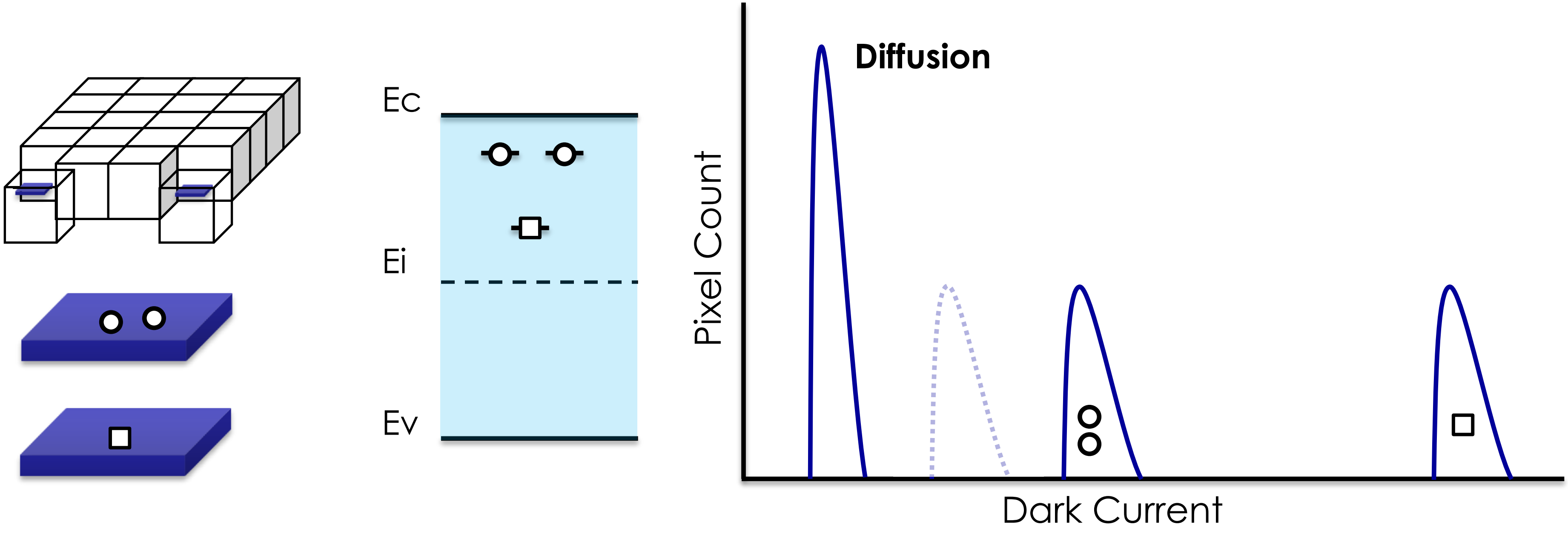

Dark Current Spectroscopy (DCS)

- DCS is used to charaterize radiation induced defects throughout the dark current distribution of all the pixels of the matrix.
- The per pixel dark current relies on silicon sampled by the PPD depleted volume.

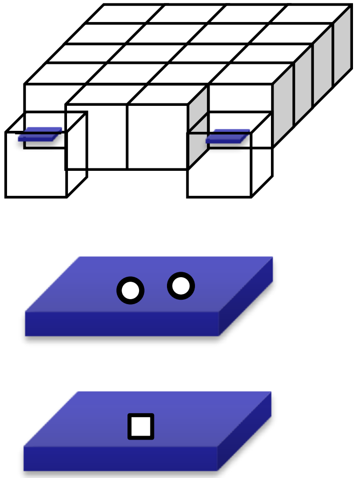

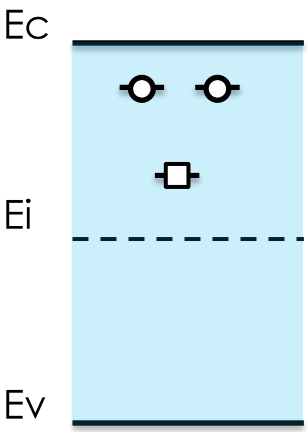

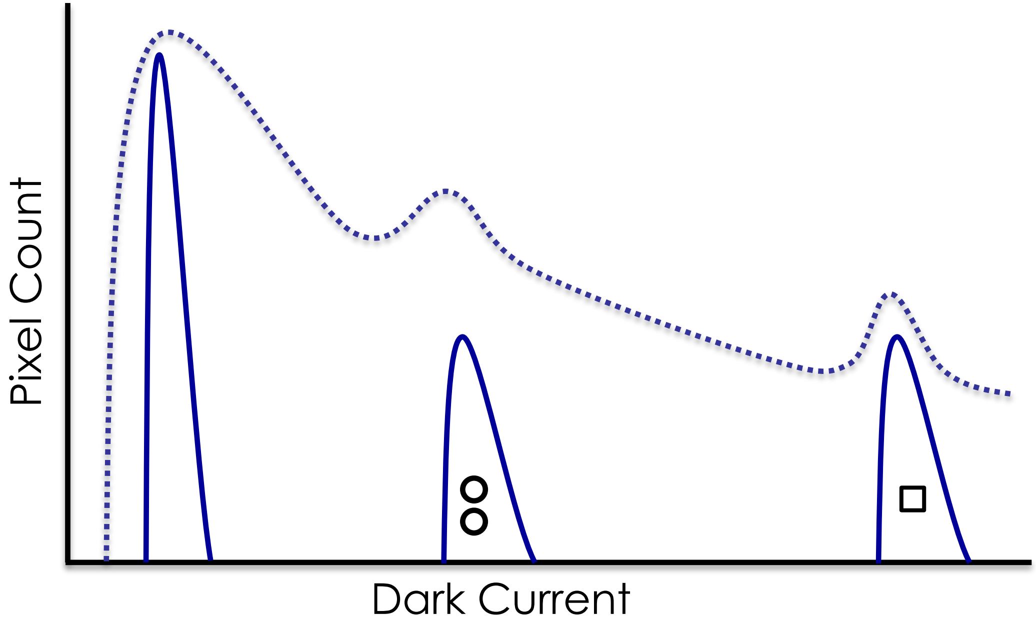

Dark Current Spectroscopy (DCS)

- The generation dark current expression of a stable defect with energy level $\boldsymbol{E_t}$ is given by:

$$I_{dc} \approx A\,.\exp\left(-\frac{\frac{E_g}{2} - |\boldsymbol{E_t} - E_i|}{k_B\,.T}\right)$$

E_g	Silicon band GAP
E_t	Defect energy level
E_i	Silicon mid-GAP
k_B	Boltzmann Constant
T	Temperature

- The dark current temperature evolution leads to defect activation energy estimation labeled $\boldsymbol{E_a}$ with the Arrhenius law.

$$I_{dc} \approx A\,.e^{\frac{-\boldsymbol{E_a}}{k_B\,.T}} \qquad \boldsymbol{E_a} \approx \frac{E_g}{2} - |\boldsymbol{E_t} - E_i|$$

COTS Imager

- The CIS under test is a (Commercial Off-The-Shelf) COTS imager
  - 2048×2048 pixels
  - 0.18µm technology
  - 8T-PPD
  - Global shutter
  - 5.5 µm pitch pixels
  - PPD depleted volume of 5µm³

- This CIS is integrated in a microcamera for CNES space missions.

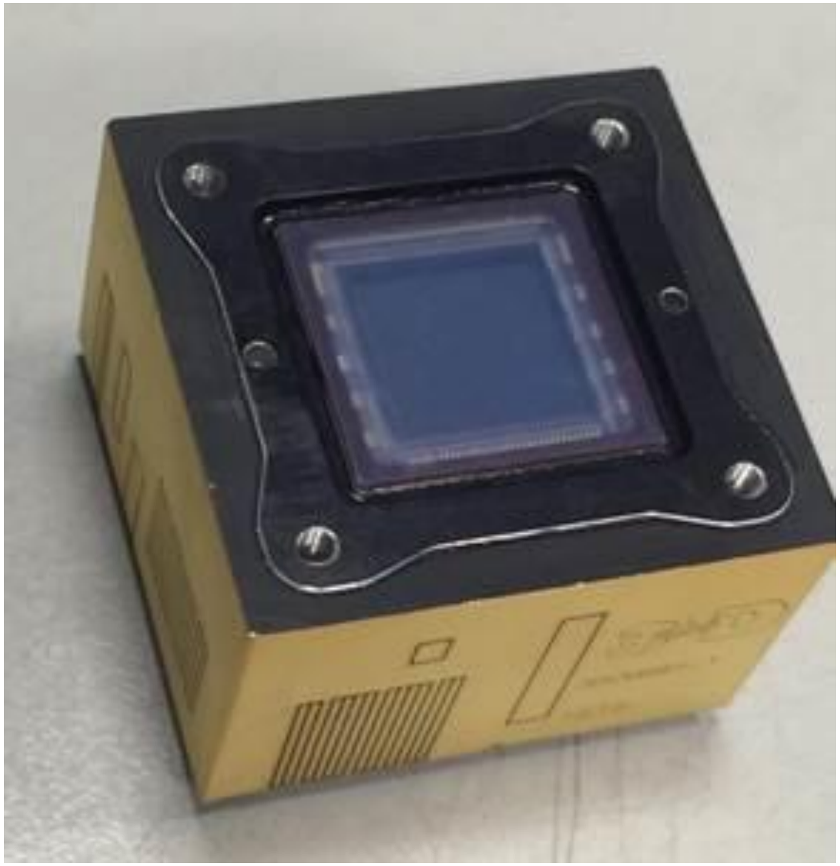

Dark Current distribution Before Irradiation

- Dark current and activation energy distribution plotted at 30°C

  - Diffusion peak containing pixels without defect in the microvolume.

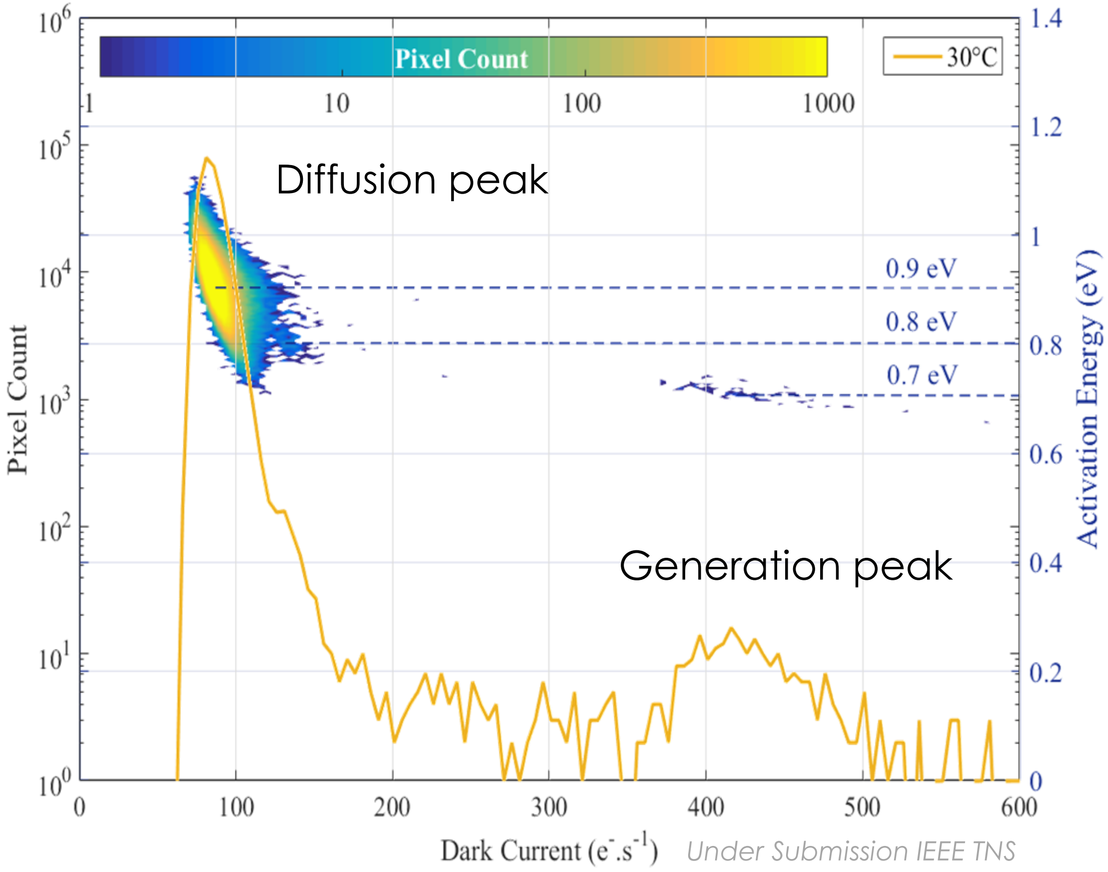

Under Submission IEEE TNS

Dark Current distribution Before Irradiation

- Dark current and activation energy distribution plotted at 30°C

  - Diffusion peak containing pixels without defect in the microvolume.
  - Generation peak due to CMOS foundry process.

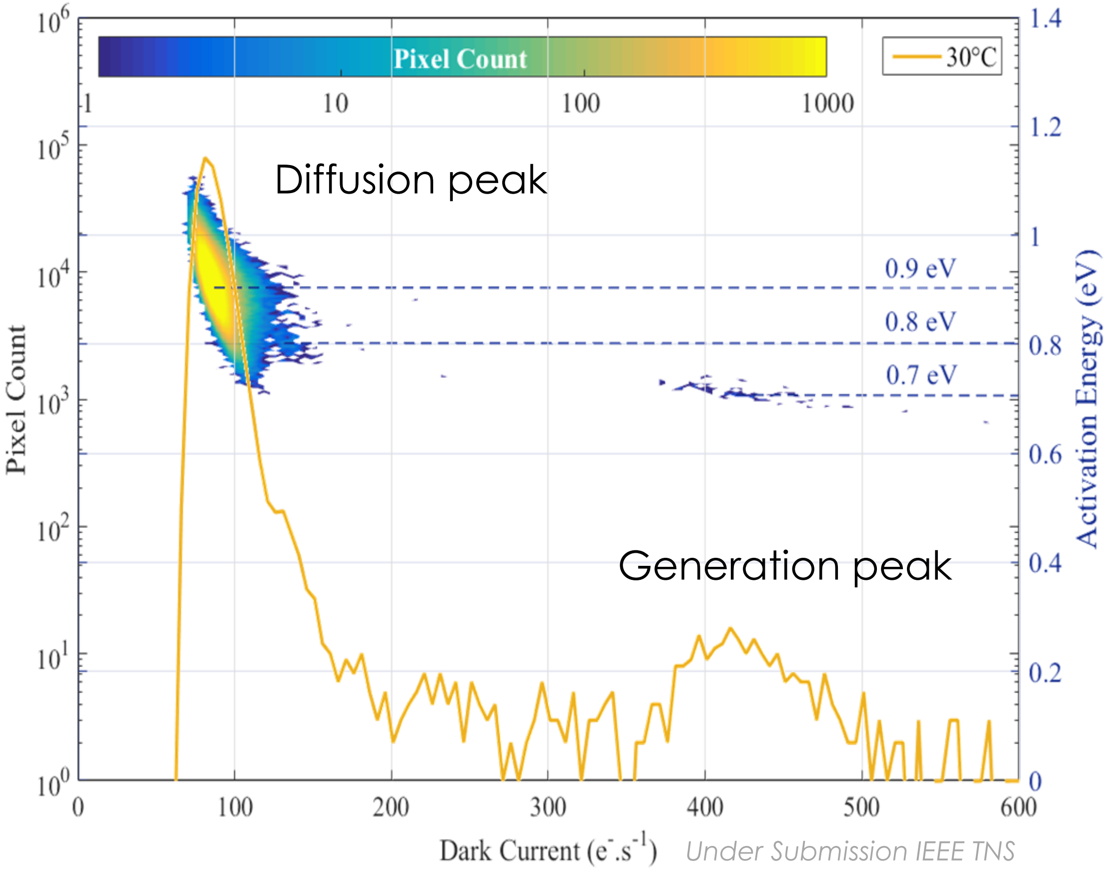

Under Submission IEEE TNS

Irradiations Parameters (20°C)

- High energy proton (A-50MeV B-150 MeV)
  - Nuclear chocs
  - **Cascade of defects**

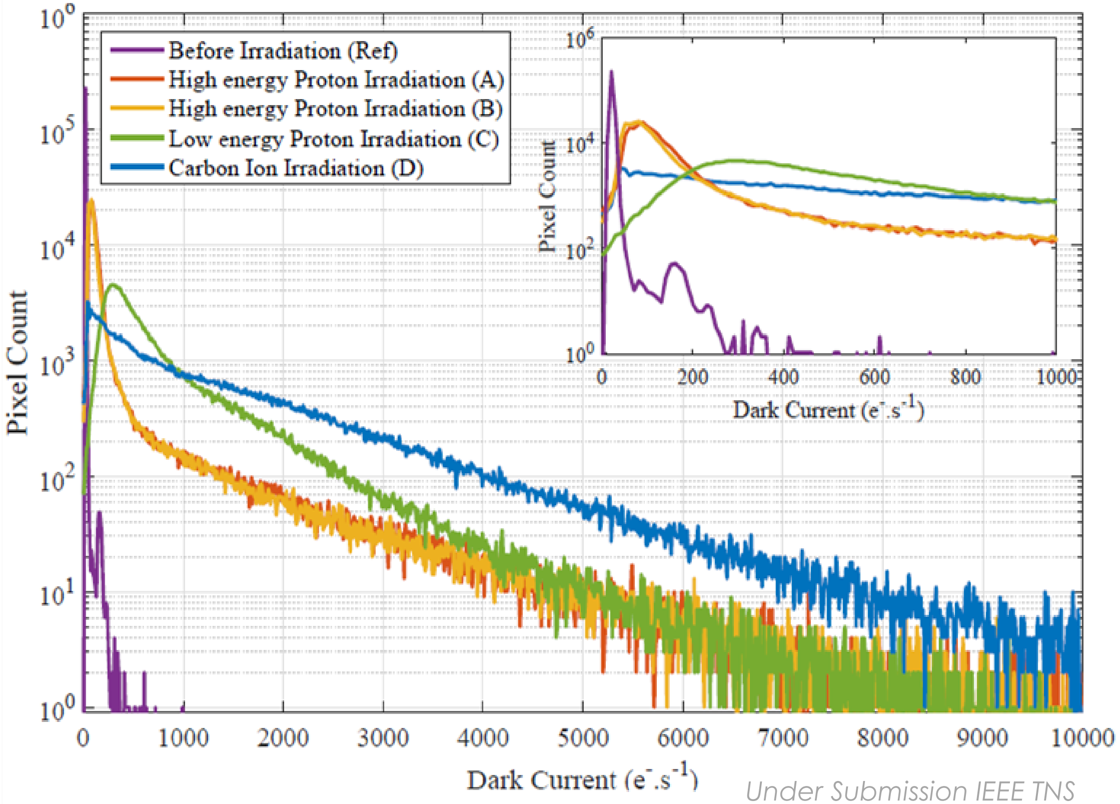

Under Submission IEEE TNS

Irradiations Parameters (20°C)

- High energy proton (A-50MeV B-150 MeV)
  - Nuclear chocs
  - **Cascade of defects**
- Carbon ion (D-10 MeV)
  - Nuclear chocs and Coulombic interaction
  - **Cascade of defects and Point defects**

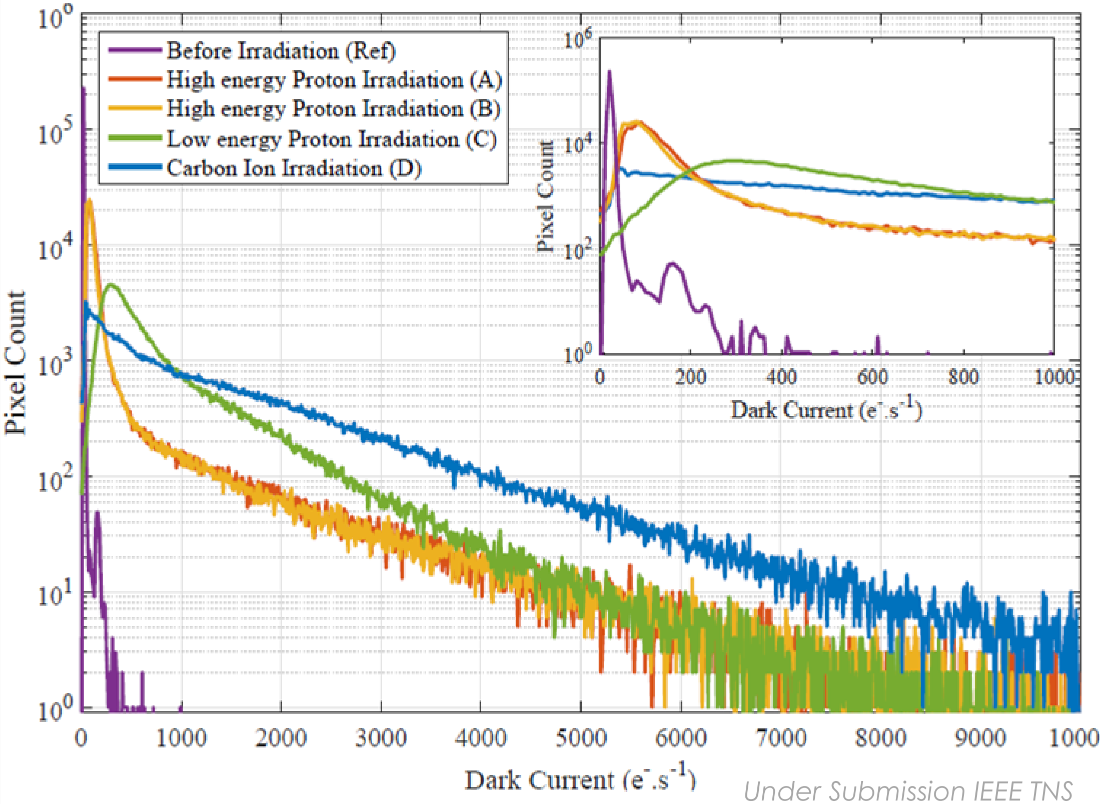

Under Submission IEEE TNS

Irradiations Parameters (20°C)

- High energy proton (A-50MeV B-150 MeV)
  - Nuclear chocs
  - **Cascade of defects**
- Carbon ion (D-10 MeV)
  - Nuclear chocs and Coulombic interaction
  - **Cascade of defects and Point defects**
- Low energy proton (C-1 MeV)
  - Coulombic interaction
  - **Point defects**
  - **Best case for the Dark Current Spectroscopy technique**

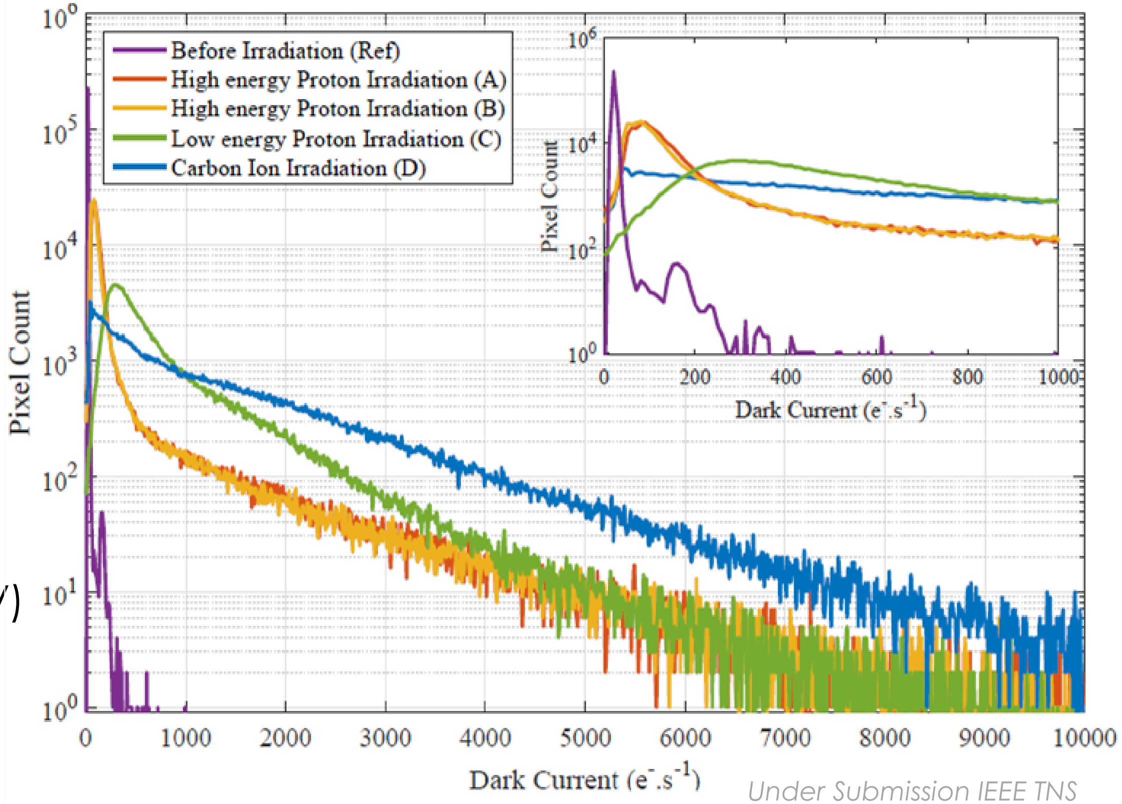

Under Submission IEEE TNS

High Energy Proton

1
High-energy proton

2
Carbon ion

3
Low energy proton

- Dark current distribution evolution with annealings plotted at 20°C

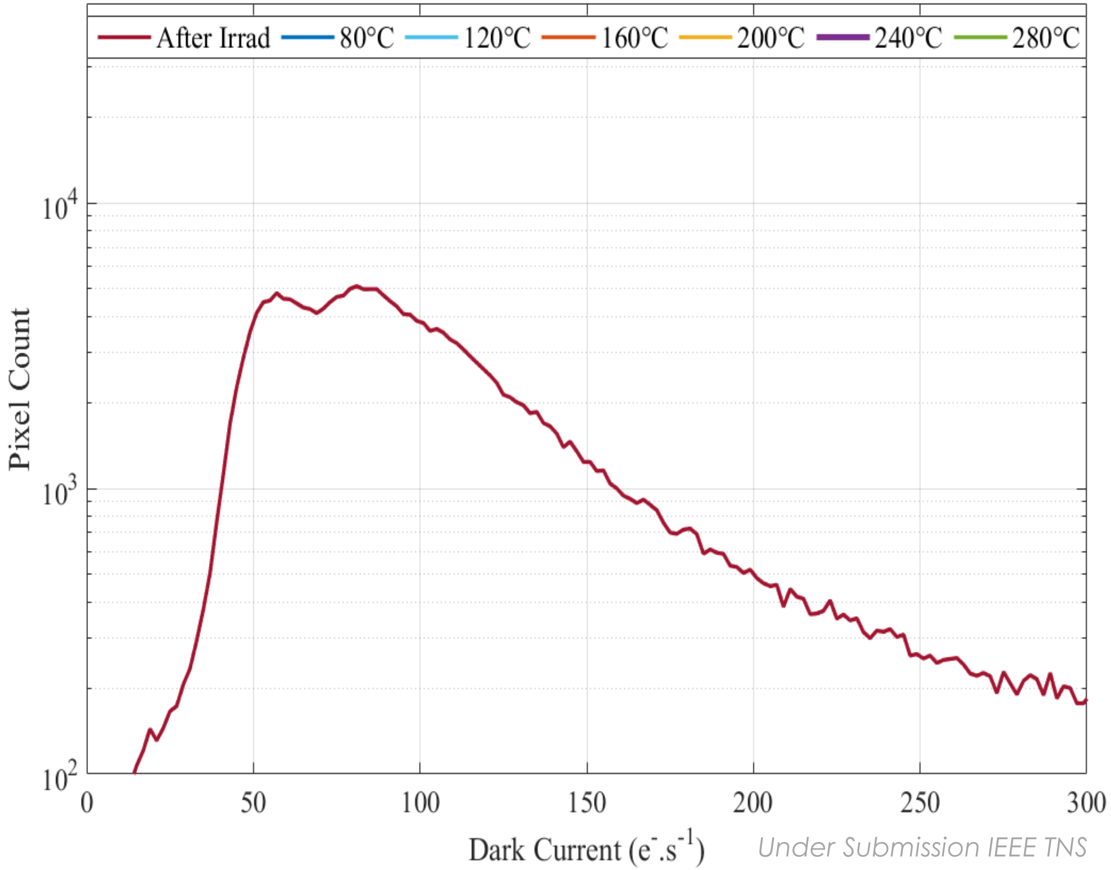

Under Submission IEEE TNS

High Energy Proton

1
High-energy proton

2
Carbon ion

3
Low energy proton

- Dark current distribution evolution with annealings plotted at 20°C

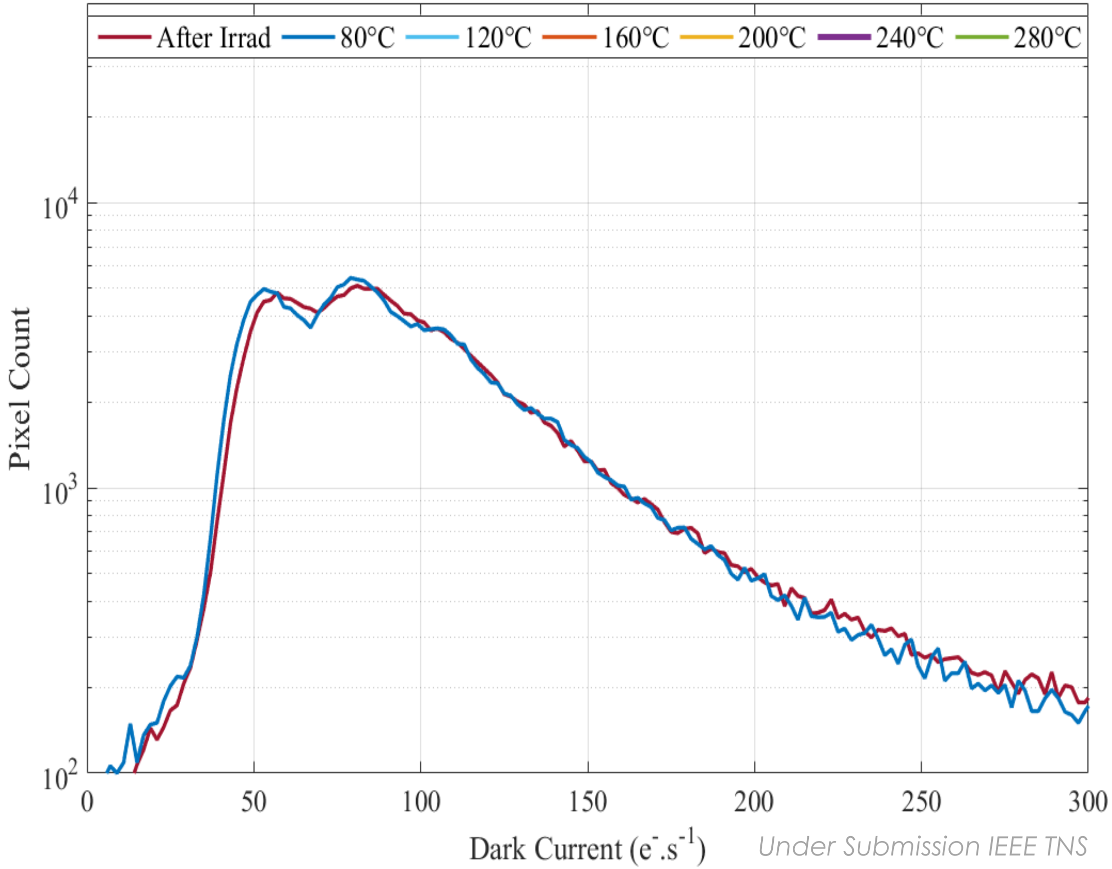

Under Submission IEEE TNS

High Energy Proton

1 High-energy proton

2 Carbon ion

3 Low energy proton

- Dark current distribution evolution with annealings plotted at 20°C

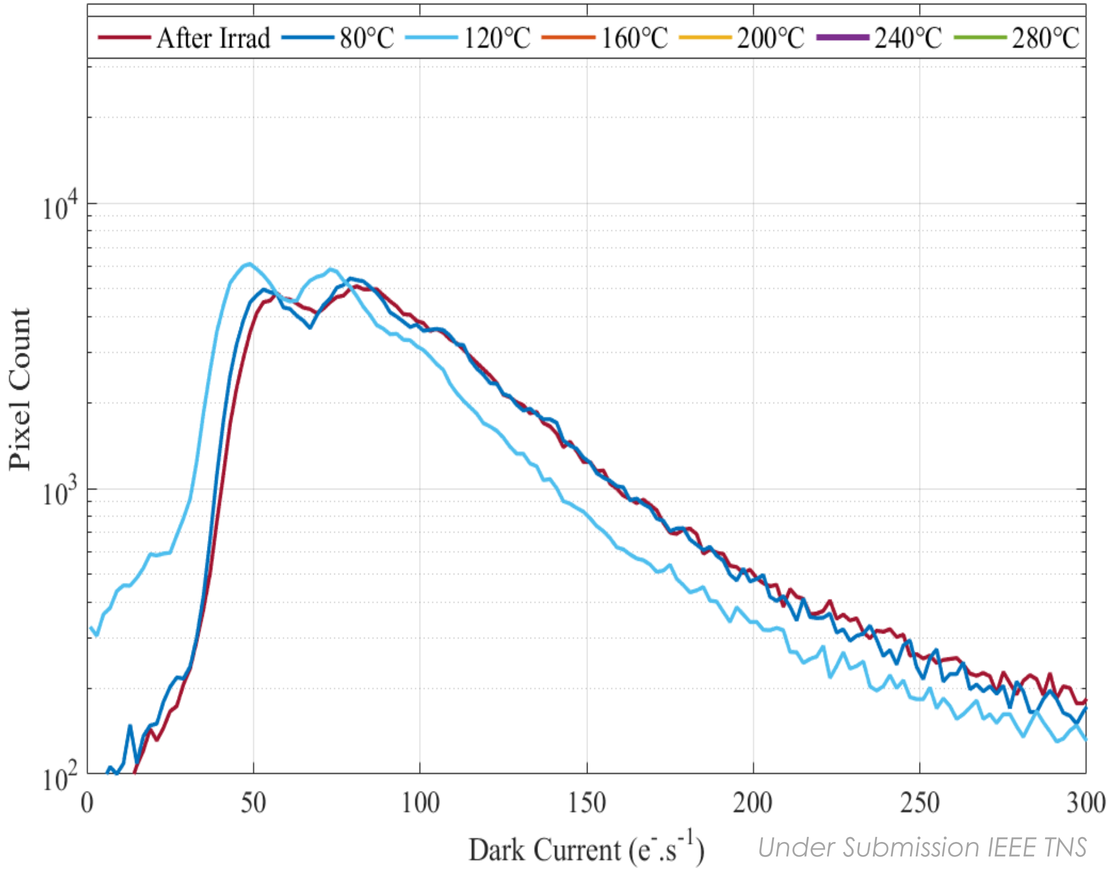

Under Submission IEEE TNS

High Energy Proton

1
High-energy proton

2
Carbon ion

3
Low energy proton

- Dark current distribution evolution with annealings plotted at 20°C

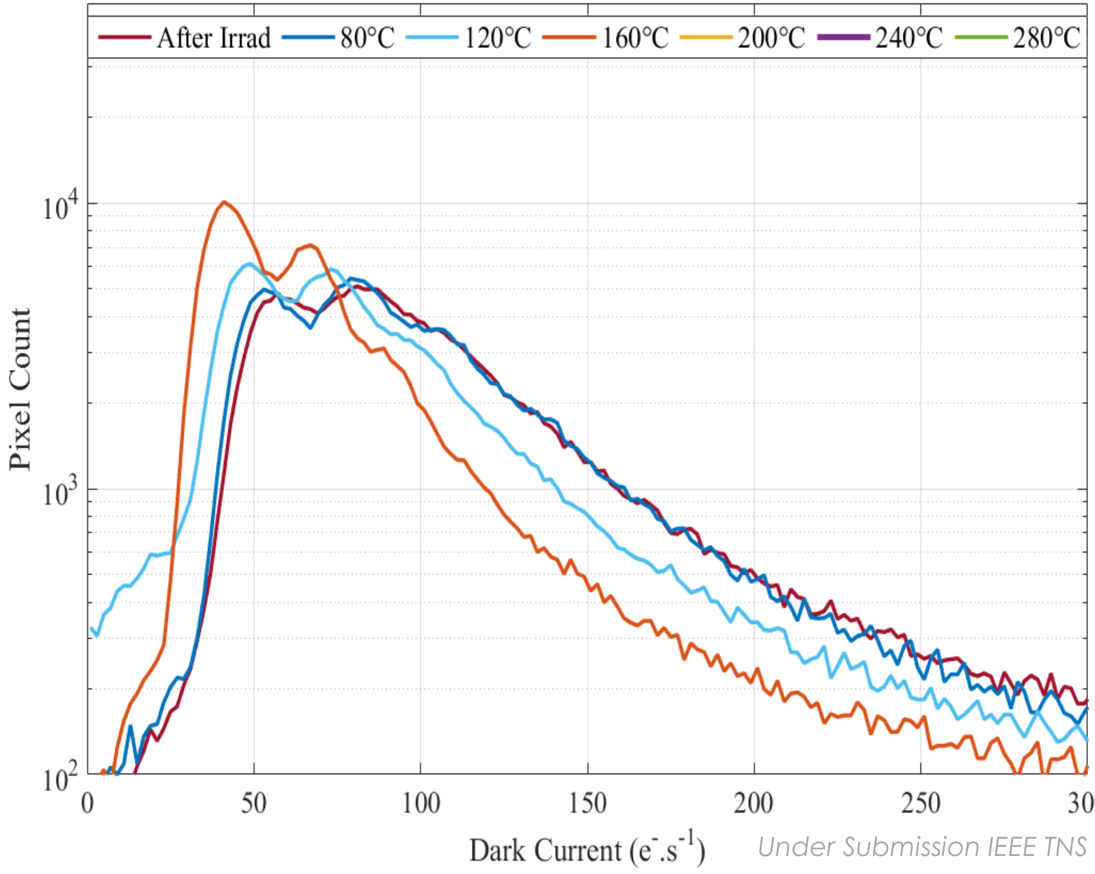

Under Submission IEEE TNS

High Energy Proton

1
High-energy proton

2
Carbon ion

3
Low energy proton

- Dark current distribution evolution with annealings plotted at 20°C

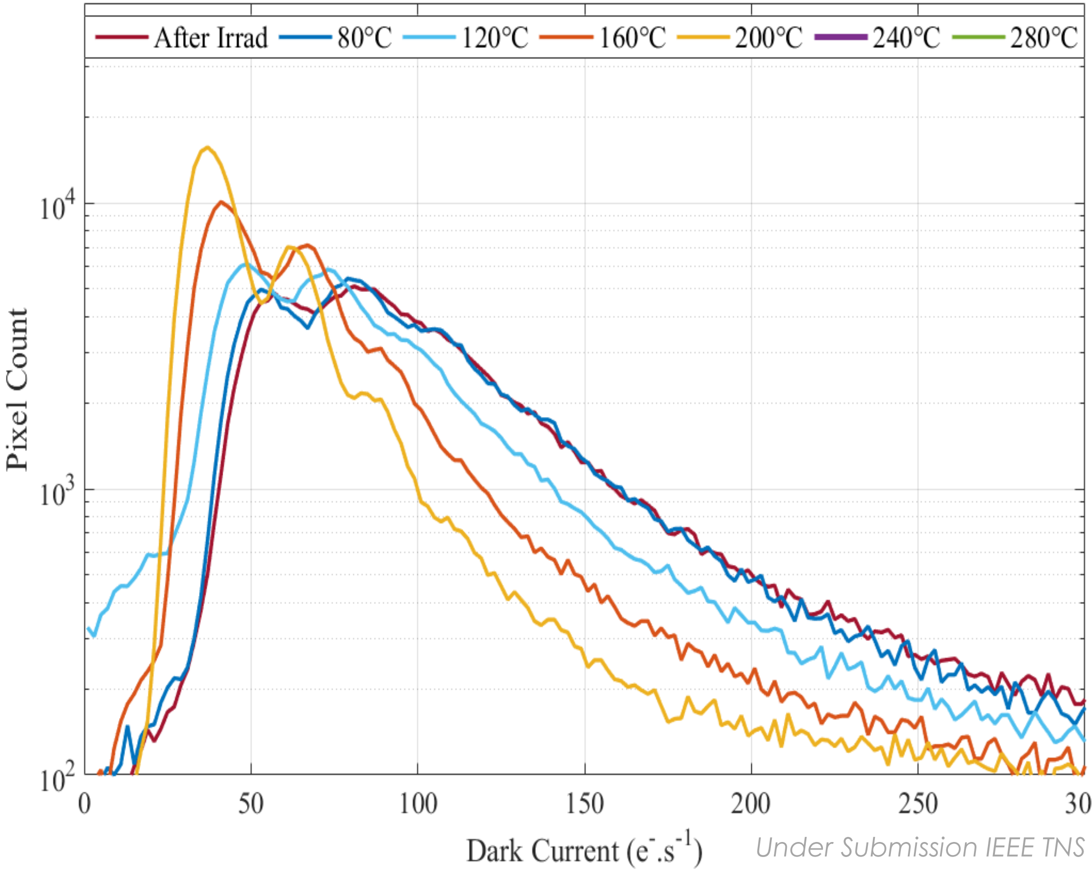

Under Submission IEEE TNS

High Energy Proton

- Dark current distribution evolution with annealings plotted at 20°C

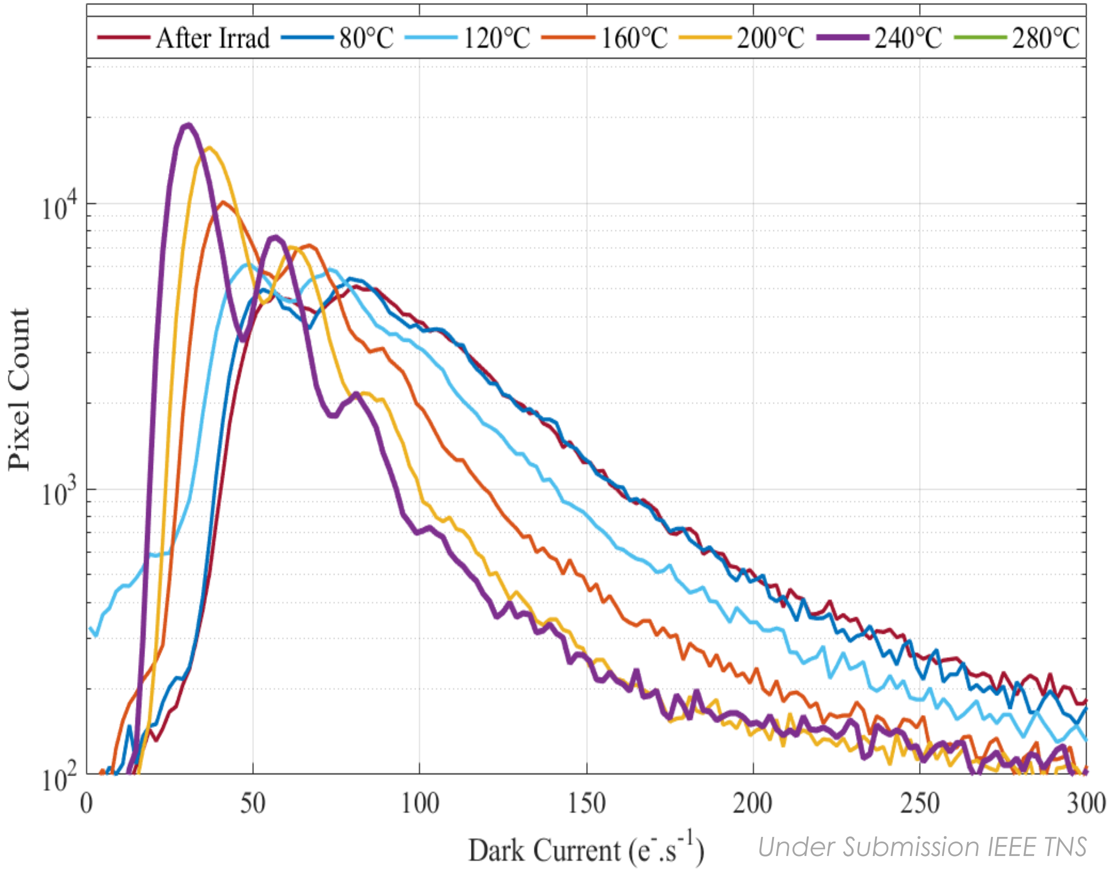

Under Submission IEEE TNS

High Energy Proton

1
High-energy proton

2
Carbon ion

3
Low energy proton

- Dark current distribution evolution with annealings plotted at 20°C

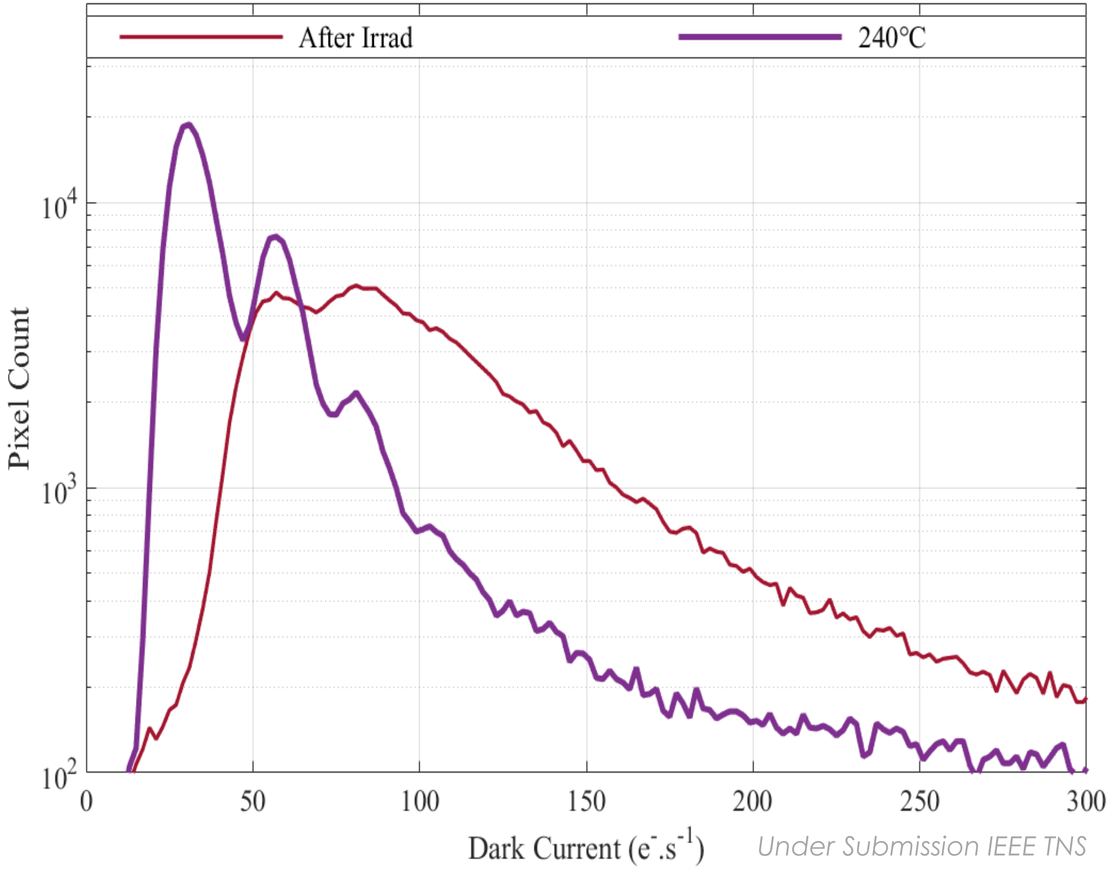

Under Submission IEEE TNS

High Energy Proton

- Dark current distribution evolution with annealings plotted at 20°C
  - TID annealing

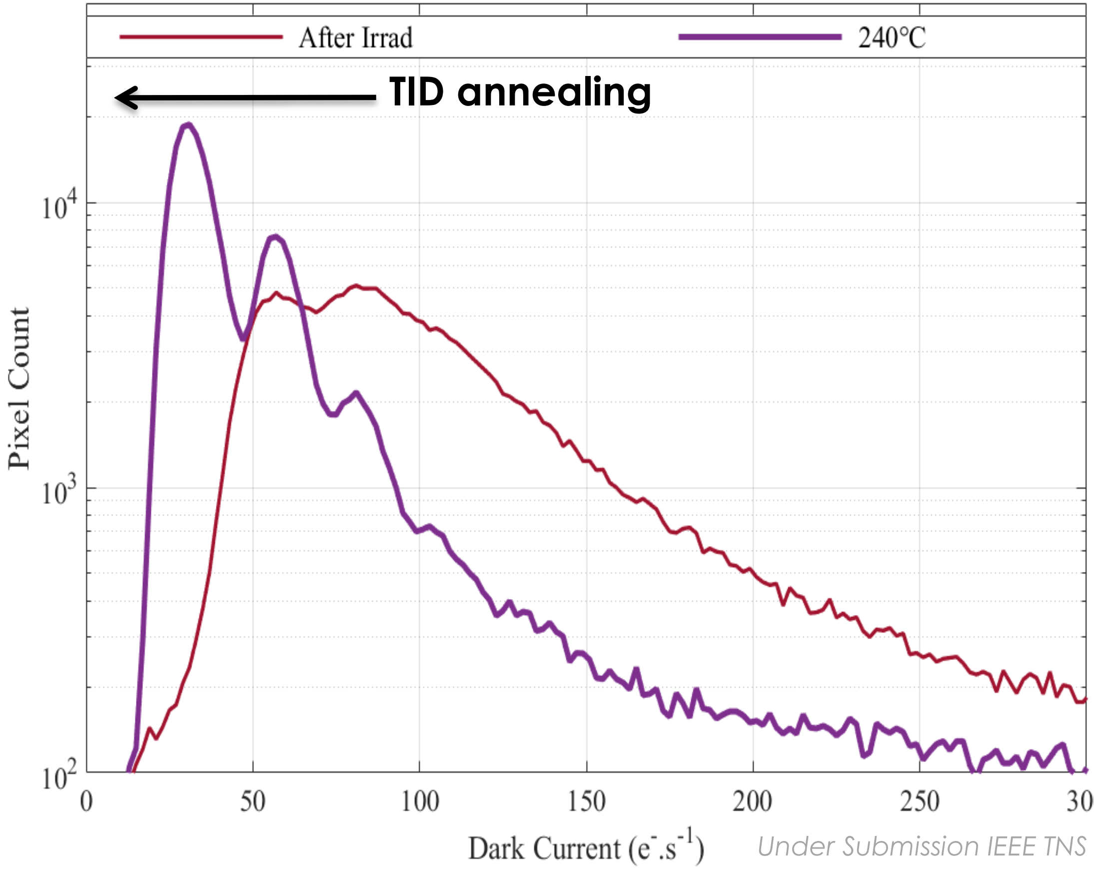

Under Submission IEEE TNS

High Energy Proton

1
High-energy proton

- Dark current distribution evolution with annealings plotted at 20°C
  - TID annealing
  - Increase of the diffusion peak.

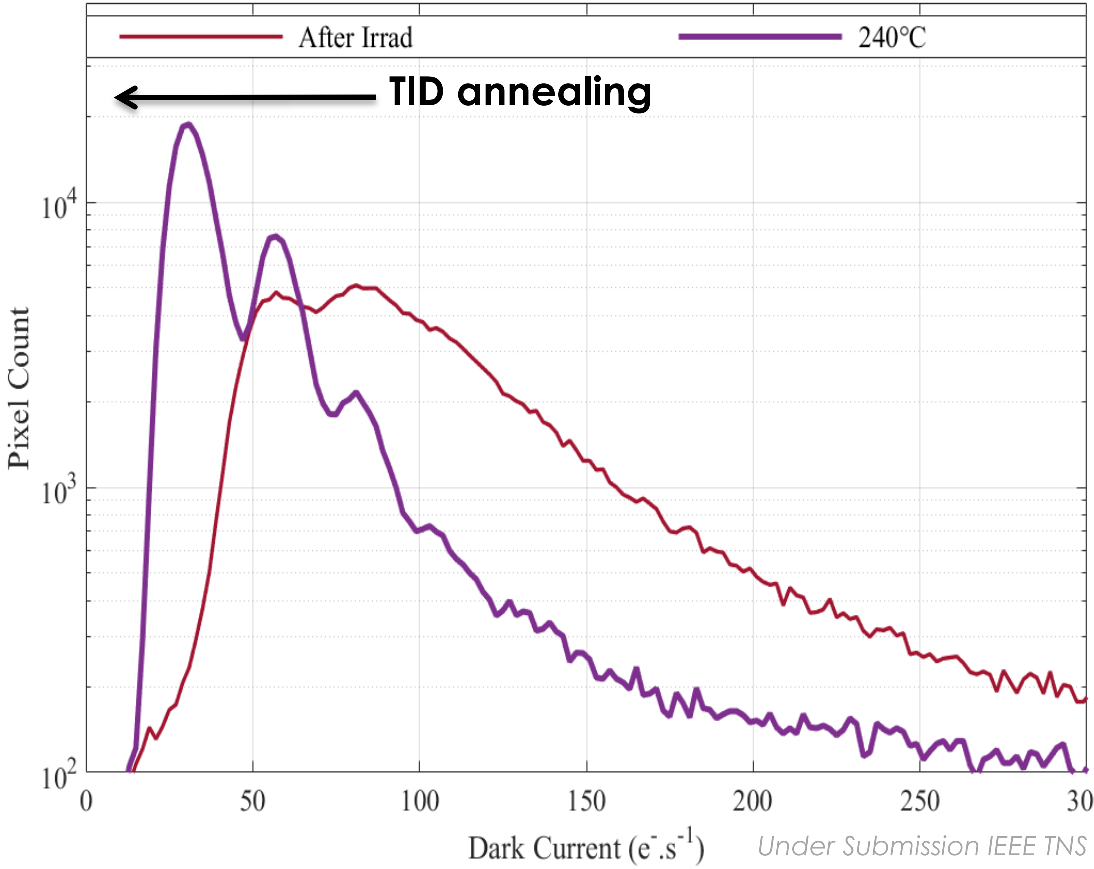

Under Submission IEEE TNS

2
Carbon ion

3
Low energy proton

High Energy Proton

1
High-energy proton

2
Carbon ion

3
Low energy proton

- Dark current distribution evolution with annealings plotted at 20°C
  - TID annealing
  - Increase of the diffusion peak.
  - Decrease of the dark current tail.

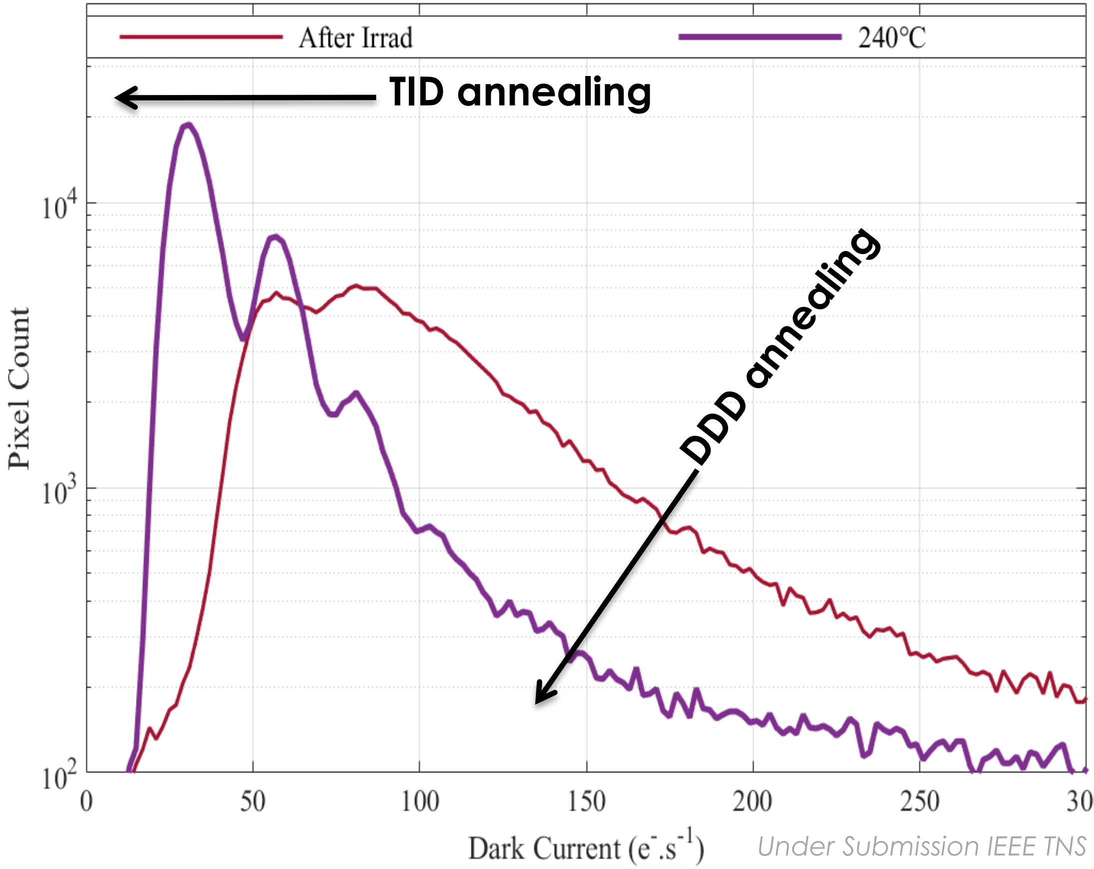

Under Submission IEEE TNS

High Energy Proton

- Dark current distribution evolution with annealings plotted at 20°C
  - TID annealing
  - Increase of the diffusion peak.
  - Decrease of the dark current tail.
  - Multiple generation peaks $\Delta I = 26$ e-/s (20°C)

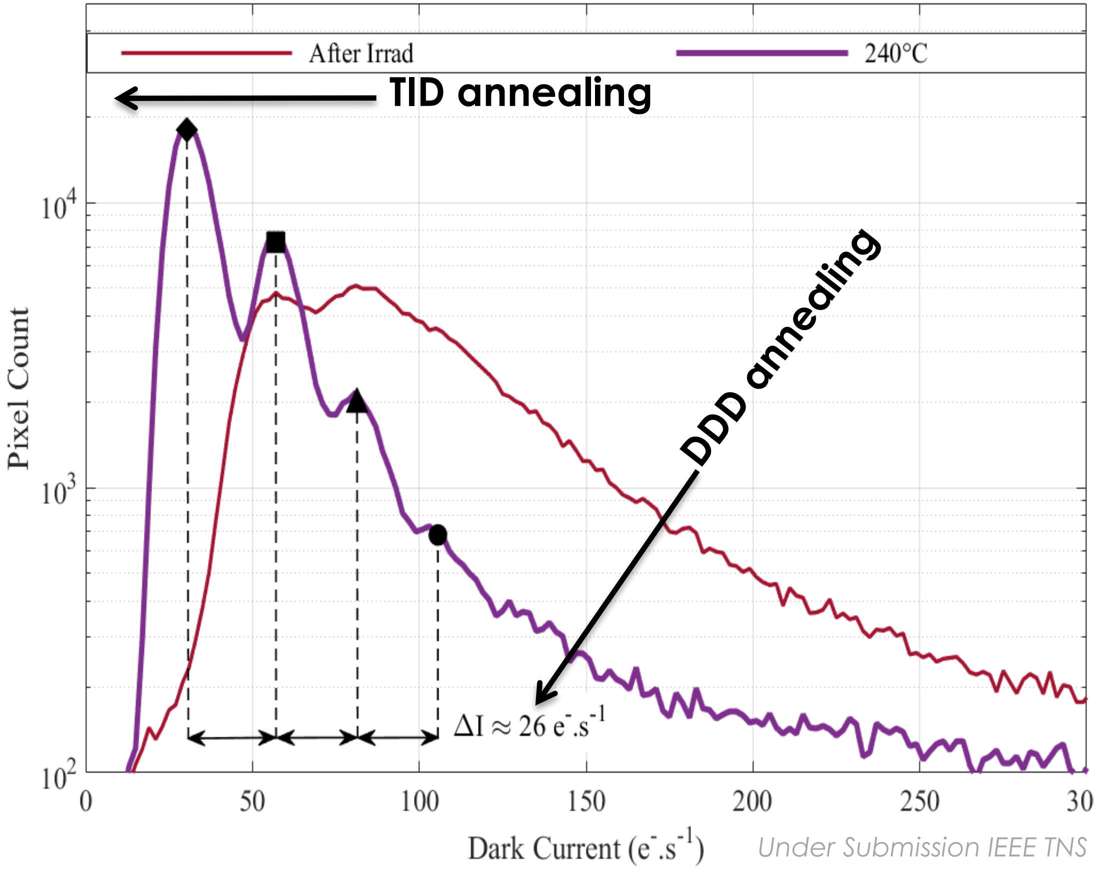

Under Submission IEEE TNS

High Energy Proton

1
High-energy proton

2
Carbon ion

3
Low energy proton

- Dark current distribution evolution with annealings plotted at 20°C

  - TID annealing
  - Increase of the diffusion peak.
  - Decrease of the dark current tail.
  - Multiple generation peaks ΔI = 26 e-/s (20°C)
  - Defect annealing between 240°C and 280°C.

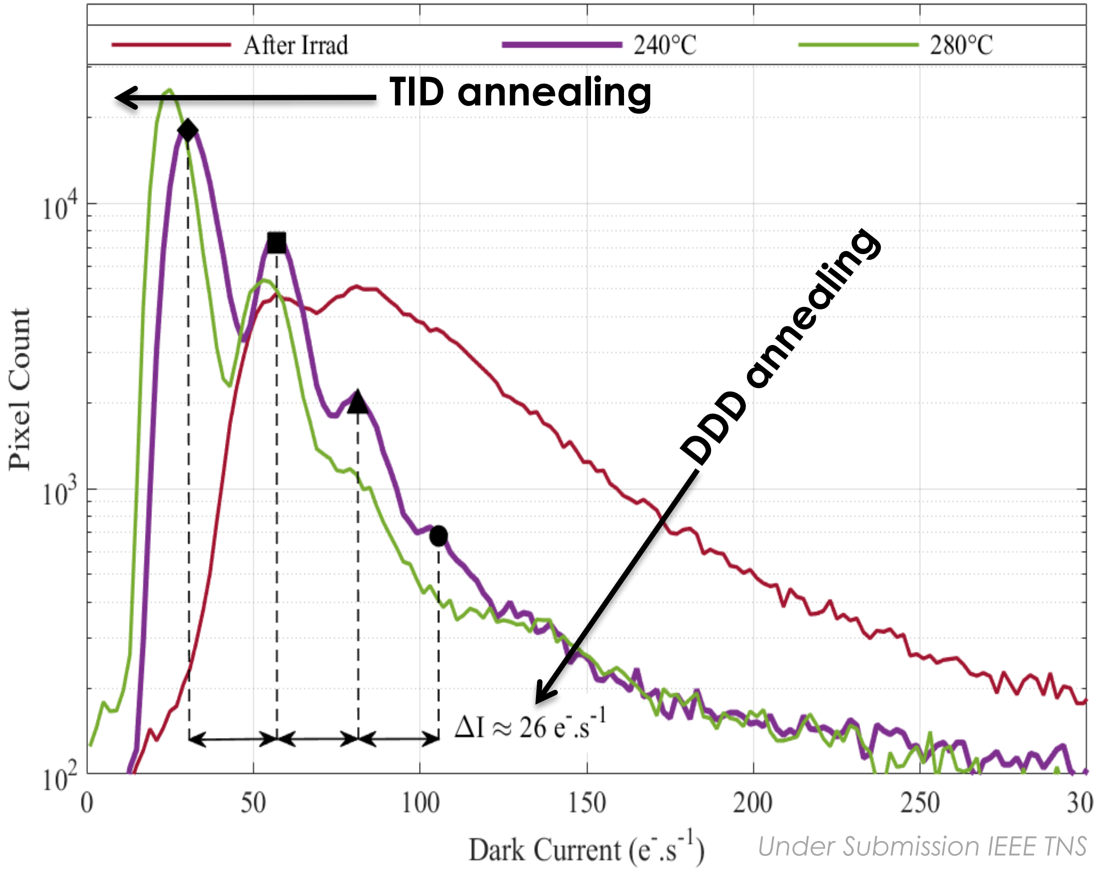

Under Submission IEEE TNS

High Energy Proton

- Activation energy evolution with annealings (240°C and 280°C)
  - Dark current **ΔI = 26 e-/s** (20°C)
  - Activation energy **Ea = 0,83eV**
  - Annealing temperature **[240°C – 280°C]**

240°C annealing

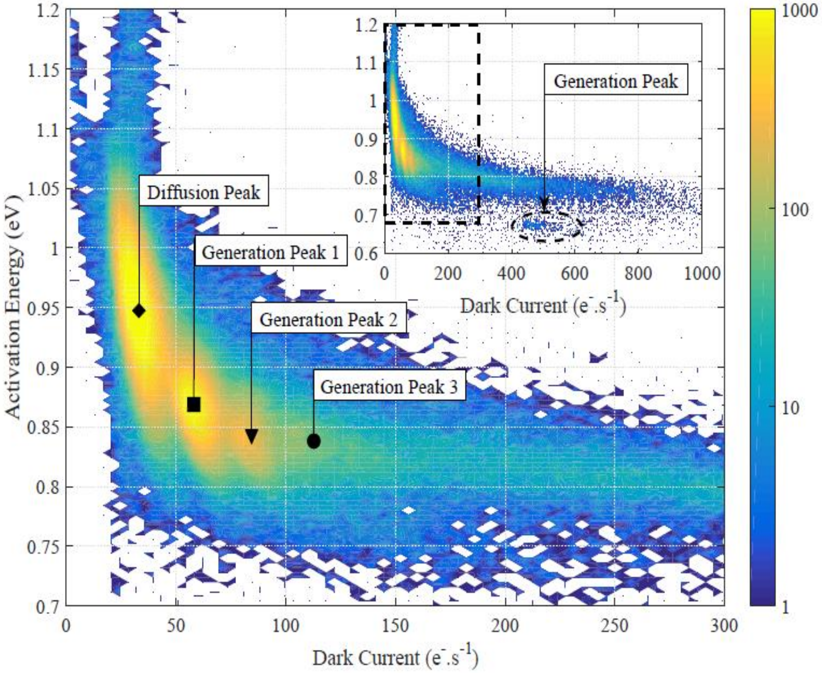

280°C annealing

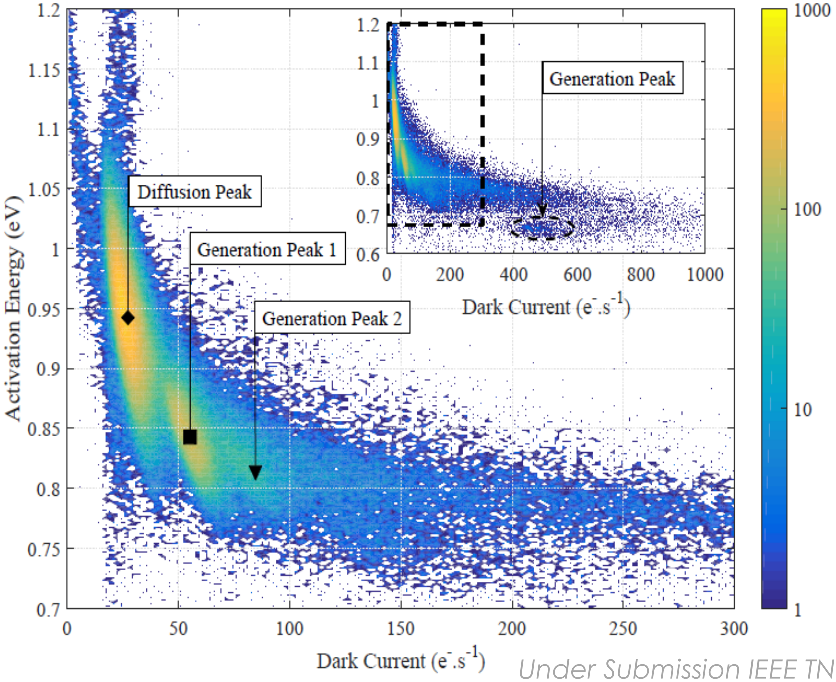

Under Submission IEEE TNS

Carbon Ion

1
High-energy proton

2
Carbon ion

3
Low energy proton

- Activation energy evolution with annealings (240°C and 280°C)
  - Dark current **ΔI = 30 e-/s** (20°C)
  - Activation energy **Ea = 0,83eV**
  - Annealing temperature **[240°C – 280°C]**

240°C annealing

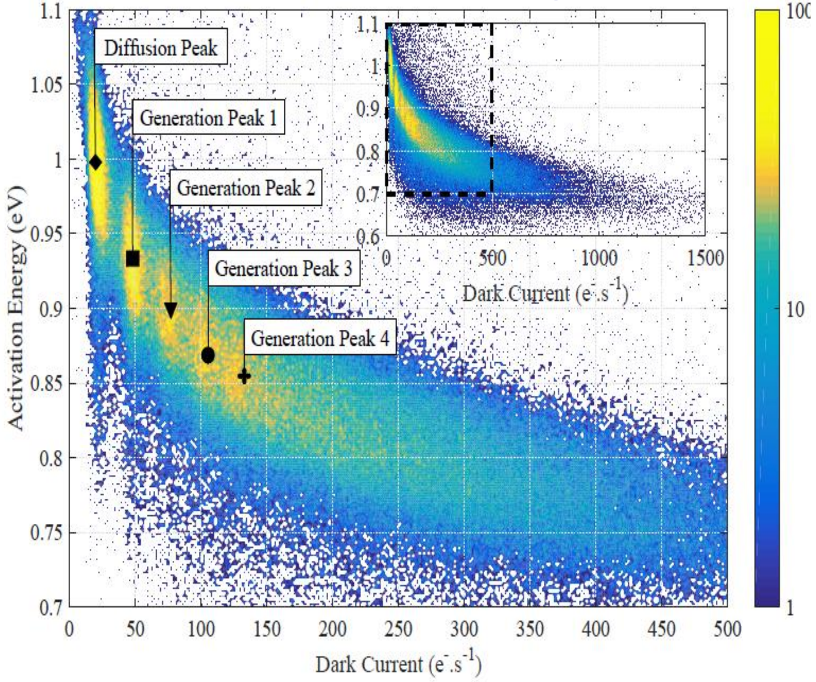

280°C annealing

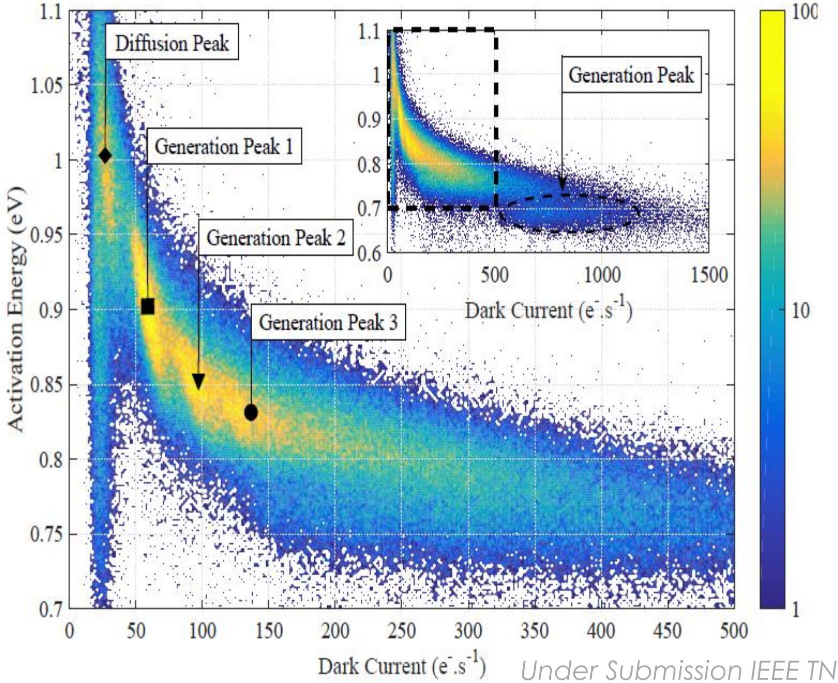

Under Submission IEEE TNS

Carbon Ion

1 High-energy proton

2 Carbon ion

3 Low energy proton

- Activation energy evolution with annealings (240°C and 280°C)
  - Dark current **ΔI = 30 e-/s** (20°C)
  - Activation energy **Ea = 0,83eV**
  - Annealing temperature **[240°C – 280°C]**

Same defects identification after high energy proton

240°C annealing

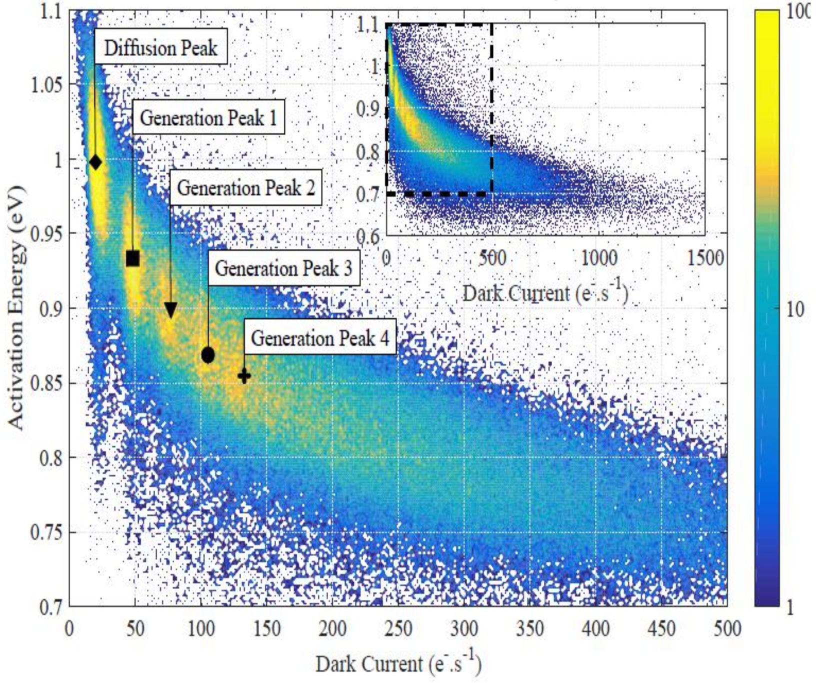

280°C annealing

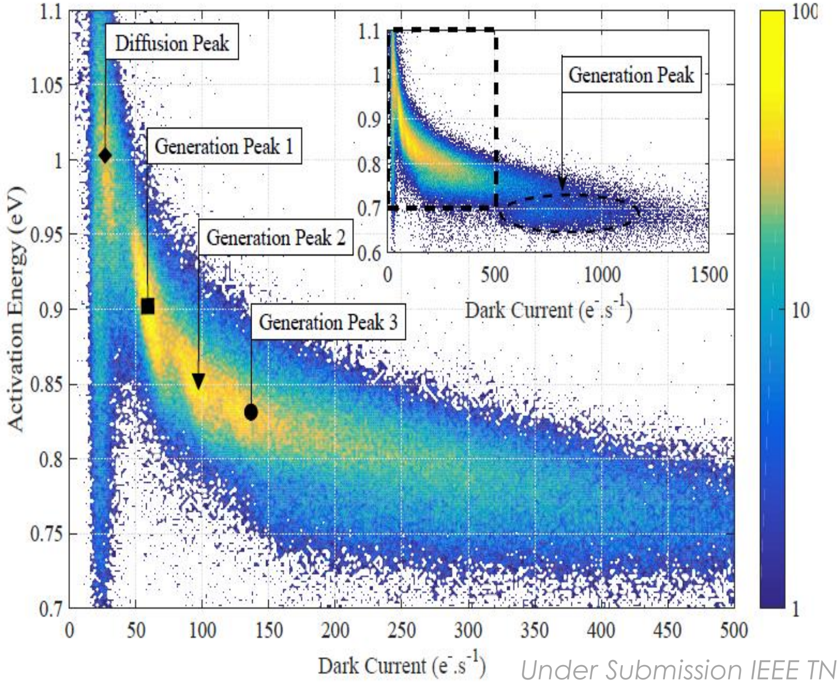

Under Submission IEEE TNS

Low Energy Proton

- Dark current distribution evolution with annealings plotted at 20°C

- TID annealing
- Increase of the diffusion peak.
- Decrease of The dark current tail.
- Generation peaks **ΔI = 500 e-/s** (20°C)
- No annealing between 240°C and 280°C.

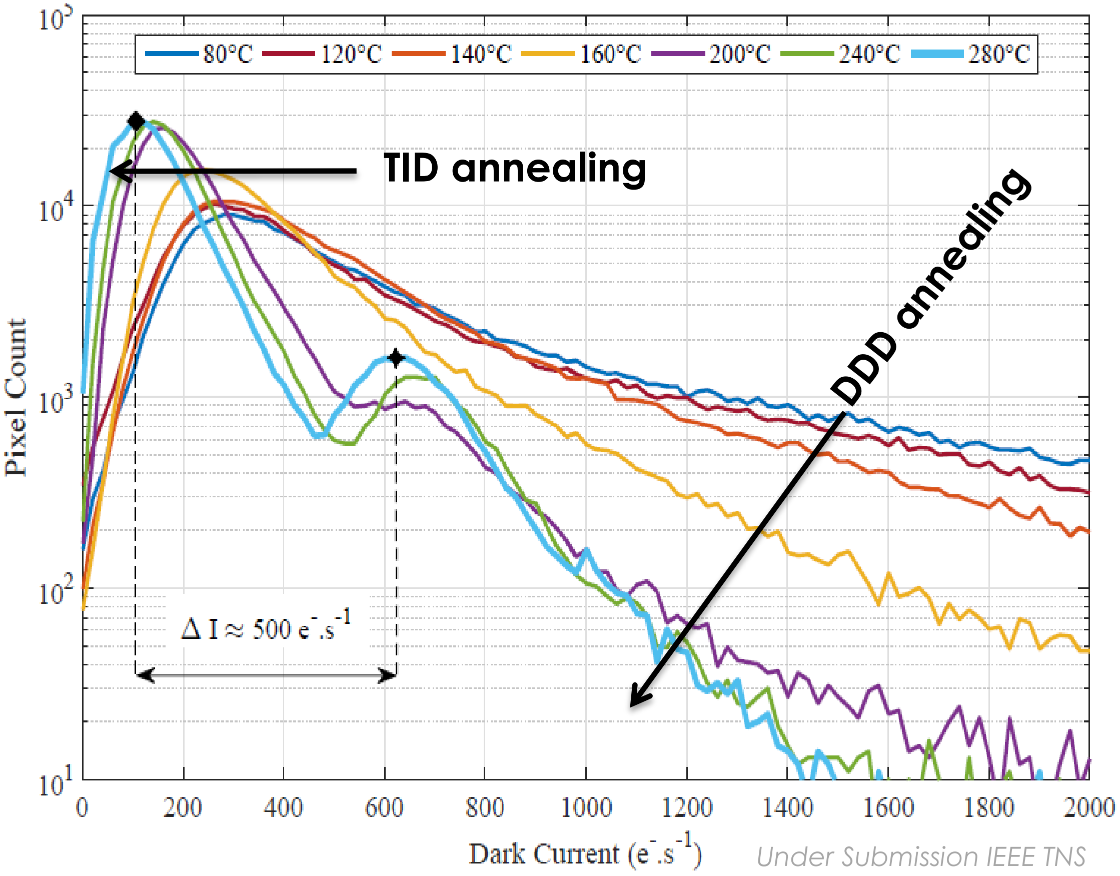

Under Submission IEEE TNS

Irradiations Comparison

Last annealing at 300°C

300°C annealing

1
High-energy proton

2
Carbon ion

3
Low energy proton

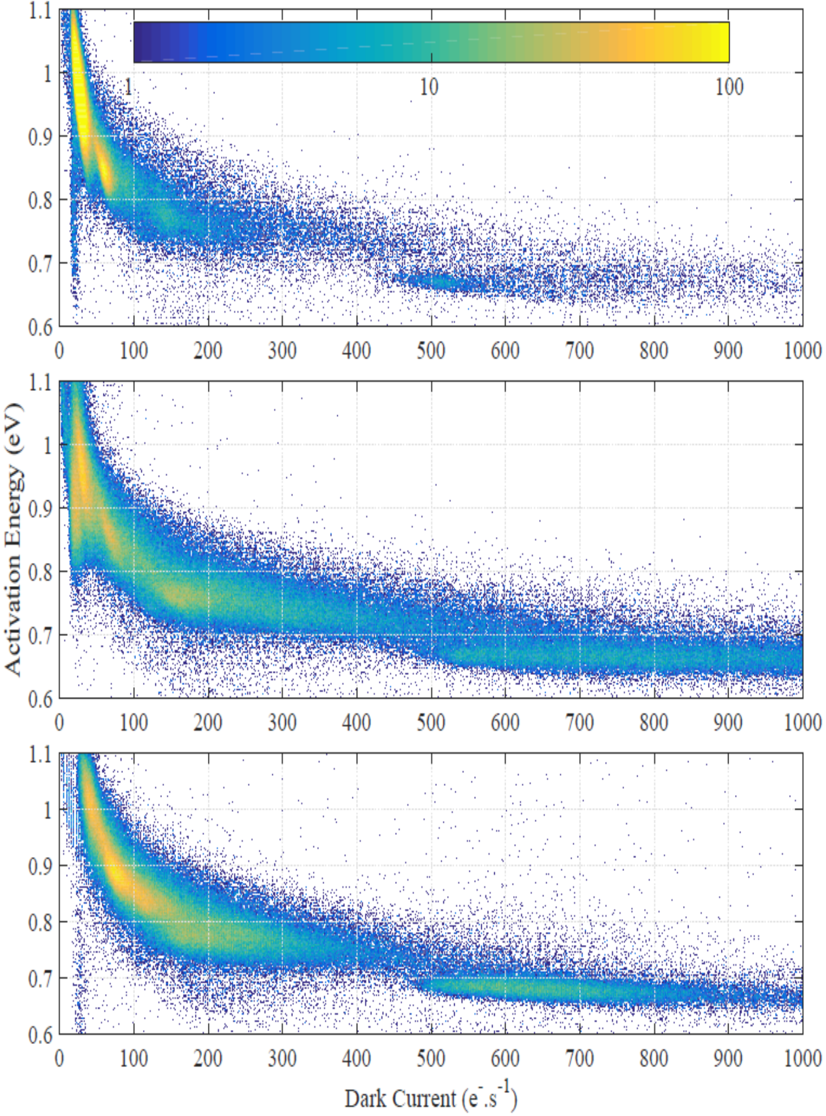

Irradiations Comparison

300°C annealing

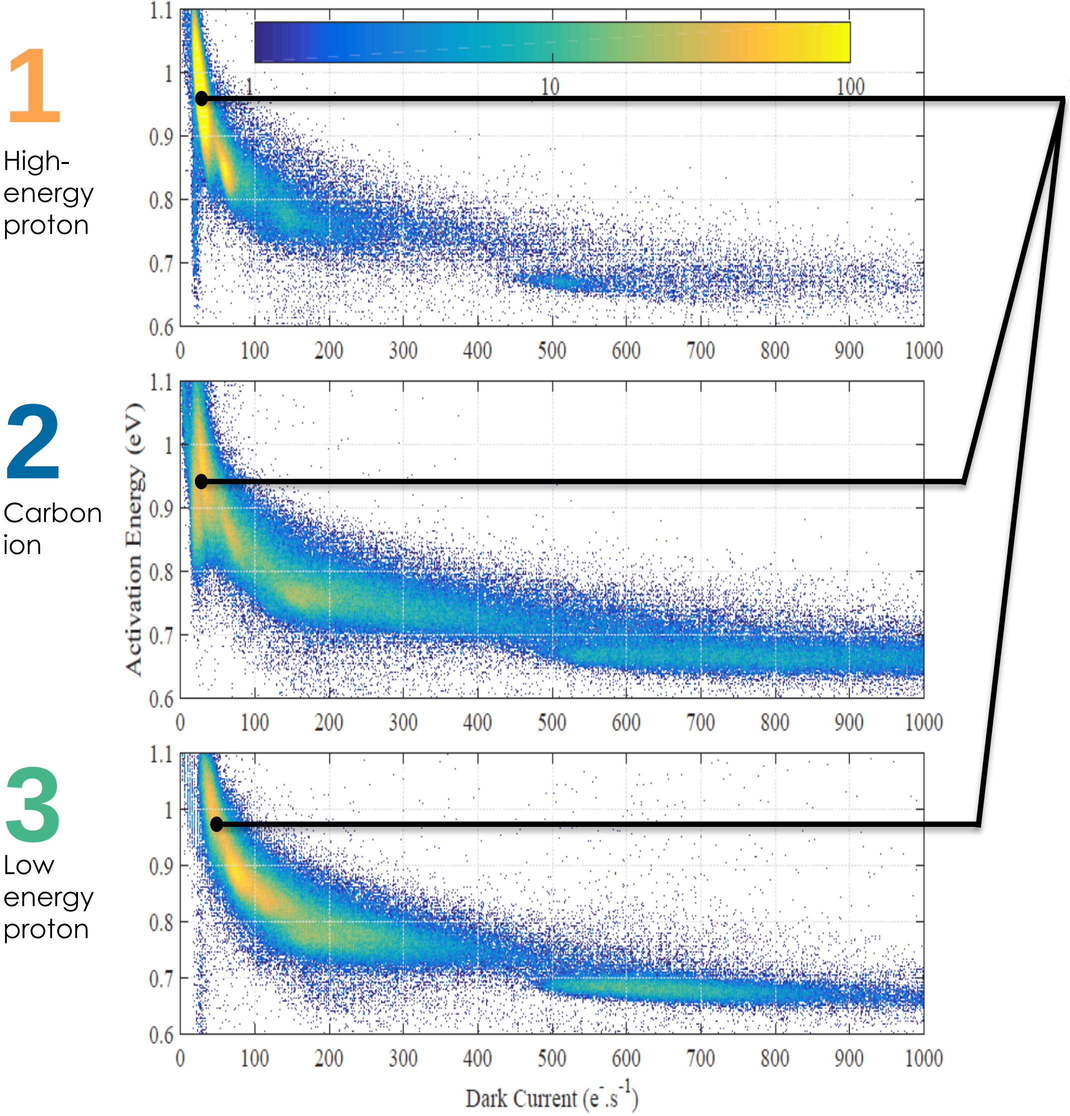

Last annealing at 300°C

- Diffusion peak
  - Idc ~ 30e-/s (20°C)
  - Ea ~ 0,95eV

Irradiations Comparison

300°C annealing

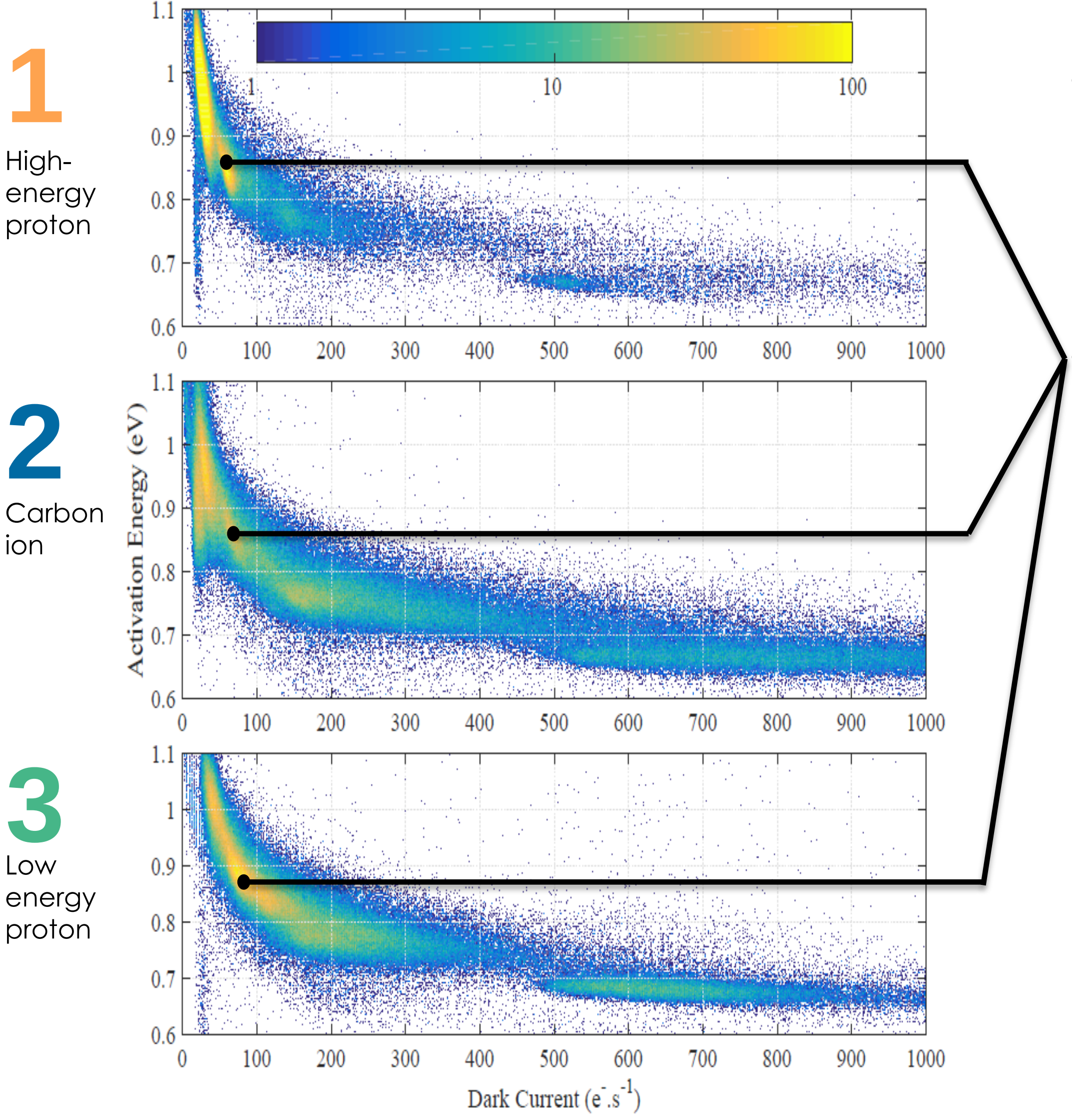

Last annealing at 300°C

- Diffusion peak
  - Idc ~ 30e-/s (20°C)
  - Ea ~ 0,95eV
- First generation peak (remaining)
  - ΔIdc ~ 30e-/s (20°C)
  - Ea ~ 0,83eV

Irradiations Comparison

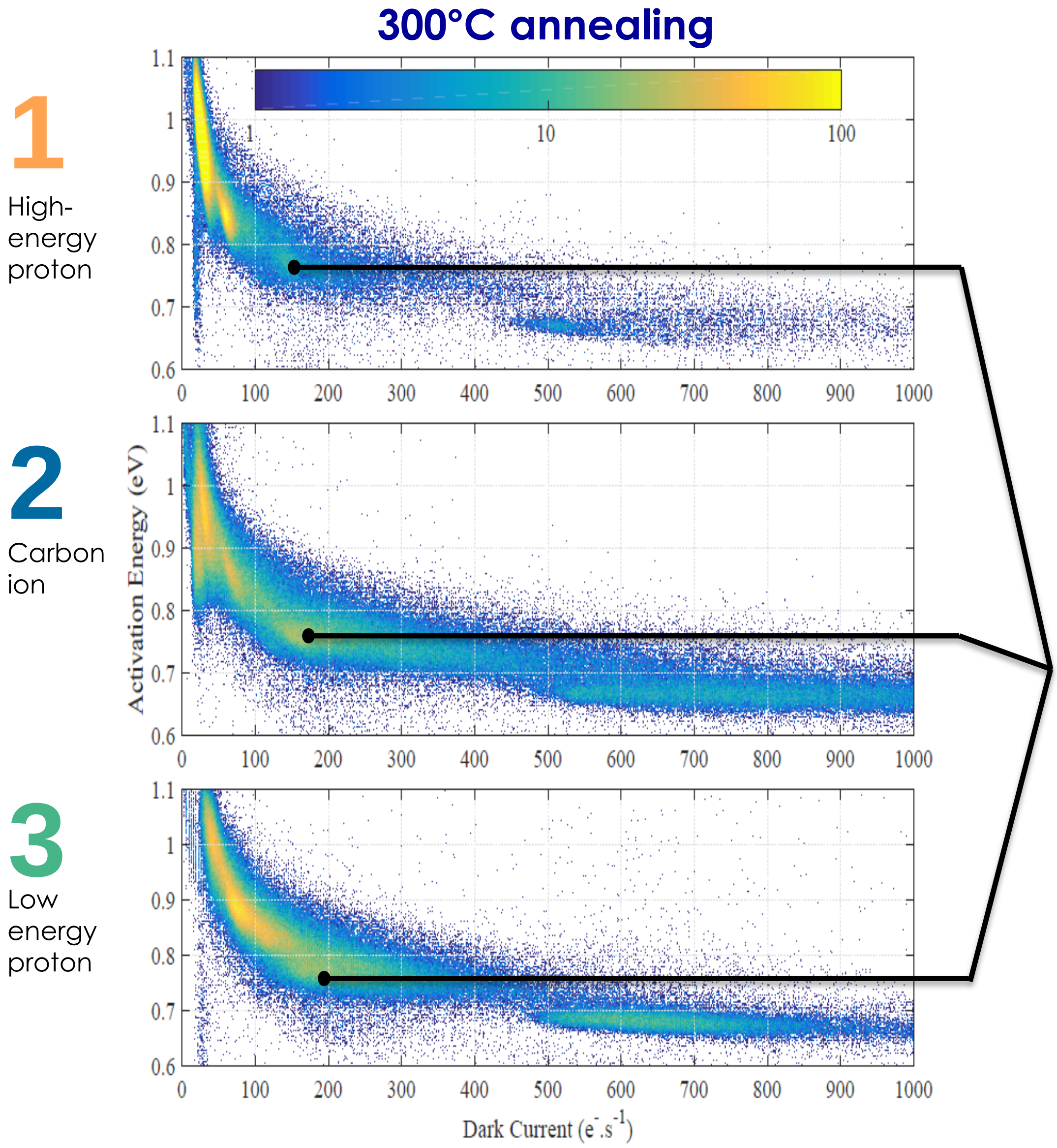

Last annealing at 300°C

- Diffusion peak
  - Idc ~ 30e-/s (20°C)
  - Ea ~ 0,95eV
- First generation peak (remaining)
  - ΔIdc ~ 30e-/s (20°C)
  - Ea ~ 0,83eV
- Second generation peak
  - Δ Idc ~ 150e-/s (20°C)
  - Ea ~ 0,75eV

Irradiations Comparison

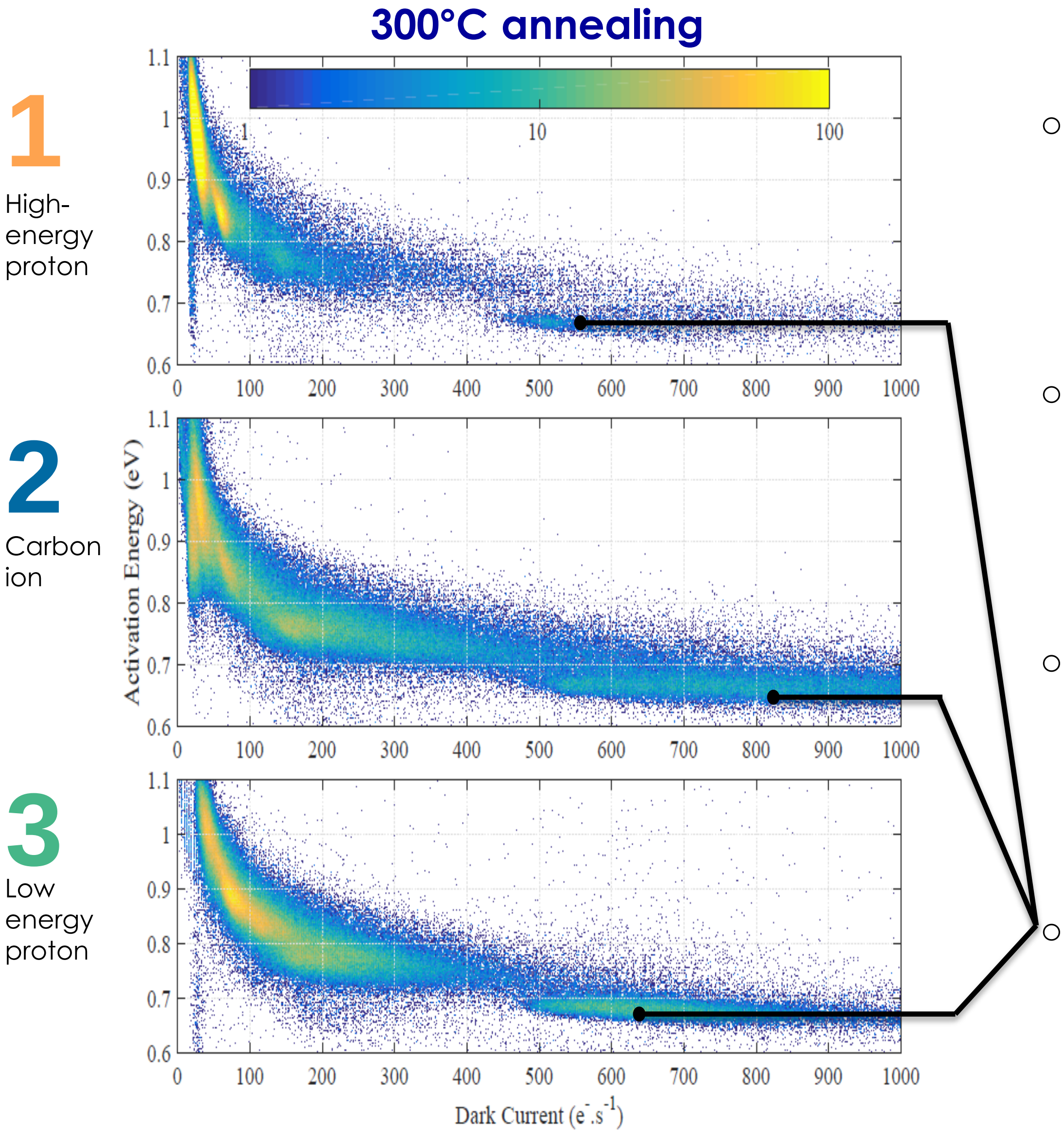

Last annealing at 300°C

- Diffusion peak
  - Idc ~ 30e-/s (20°C)
  - Ea ~ 0,95eV
- First generation peak (remaining)
  - ΔIdc ~ 30e-/s (20°C)
  - Ea ~ 0,83eV
- Second generation peak
  - ΔIdc ~ 150e-/s (20°C)
  - Ea ~ 0,75eV
- Third generation peak
  - ΔIdc ~ 600e-/s (20°C)
  - Ea ~ 0,67eV

Defects Identification and Discussion

Defect	**20°C Dark Current (e-/s)**		**$\lvert E_t-E_i \rvert$ (eV)**		**Annealing Temperature**	
Vacancy-Oxygen **VO**		-		~0,39		> 300°C
Divacancy $\mathbf{V_2}$	***~[26–30]***	~30	***~0,18***	~0,17	***[240°C–280°C]***	260°C
Divacancy-Dioxygen $\mathbf{V_2O_2}$	***150***	-	***~0,11***	~0,16	***> 300°C***	> 300°C
Vacancy-Phosphorus **VP**		~35		~0,13		150°C
Divacancy-Oxygen $\mathbf{V_2O}$	***~[500–600]***	-	***~0,01***	~0,06	***> 300°C***	> 330°C

Experimental Datas

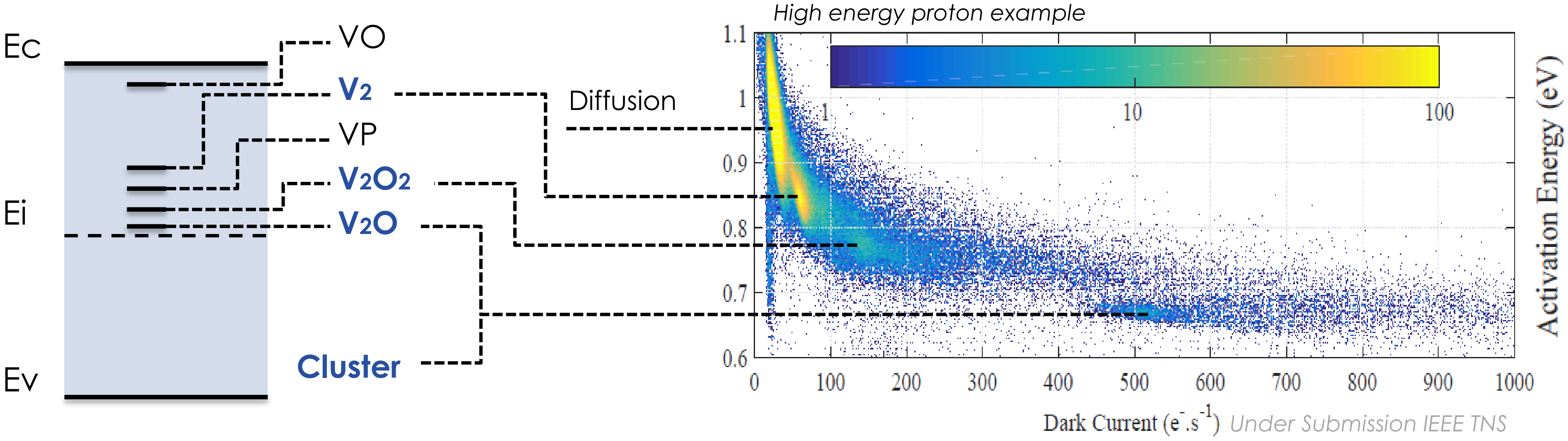

High energy proton example

Under Submission IEEE TNS

Conclusion

- 4 COTS imagers have been irradiated with:
  - High energy proton / Carbon ion / Low energy proton

Conclusion

- 4 COTS imagers have been irradiated with:
  - High energy proton / Carbon ion / Low energy proton

- The hypothetical existence of oxygen based defects such as V_2O and V_2O_2 have been pointed out.

  - The role of oxygen impurities in the dark current rise after irradiation.

Conclusion

- 4 COTS imagers have been irradiated with:
  - High energy proton / Carbon ion / Low energy proton

- The hypothetical existence of oxygen based defects such as V_2O and V_2O_2 have been pointed out.

  - The role of oxygen impurities in the dark current rise after irradiation.

Oxygen concentration ≪ Minimum impurity concentration in pure Si

Conclusion

- 4 COTS imagers have been irradiated with:
  - High energy proton / Carbon ion / Low energy proton

- The hypothetical existence of oxygen based defects such as V_2O and V_2O_2 have been pointed out.

  - The role of oxygen impurities in the dark current rise after irradiation.

Oxygen concentration ≪ Minimum impurity concentration in pure Si

- The DCS measurements suggest that similar divancancy based defects are involved in all the irradiations.

cnes
CENTRE NATIONAL D'ÉTUDES SPATIALES

ISAE
Institut Supérieur de l'Aéronautique et de l'Espace
SUPAERO

RADECS 2017
CERN, Geneva

Thanks for your attention

A. Le Roch, V. Goiffon, C. Durnez, P. Magnan
Université de Toulouse, ISAE SUPAERO, 31055 Toulouse, France.

C. Virmontois, L. Pistre, J-M. Belloir
Centre National d'Etudes Spatiales (CNES), 31400 Toulouse, France.

Irradiations Parameters

IRRADIATION PARAMETERS

Sensor Ref	A	B	# (for UDF)	C	D
Particles	Proton	Proton	Proton	Proton	Carbon
Energy (Mev)	50	150	50	1	10
Fluence (cm-2)	1,30 E+11	3,00 E+11	2,00 E+11	3.00 E+8	1.00 E+10
DDD (Tev.g-1)	504,4	645	776	+	++
TID (KradSi)	20,49	21,02	315,2	-	-

High energy proton
- Good NIEL estimation
- DDD Nuclear chocs
- Cluster of defects

Low energy proton
- Huge NIEL at End Of Range (EOR)
- Huge DDD
- Coulombic interactions
- Point defects

Carbon ion
- Huge cross section and mass
- DDD Nuclear chocs
- Cluster of defects

Universal Damage Factor (UDF)

Sensor Ref	A	B	C
Particles	Proton	Proton	Proton
Energy (Mev)	50	150	50
Fluence (cm-2)	1,30 E+11	3,00 E+11	2,00 E+11
DDD (Tev.g-1)	504,4	645	776
TID (KradSi)	20,49	21,02	315,2
ΔI (e-/s)	415	424	542

$V_{dep} = 5\mu m^3$

$K_{dark} = 1.9 \times 10^5 \ (e/\text{cm}^3.\text{s})/(\text{MeV/g})$

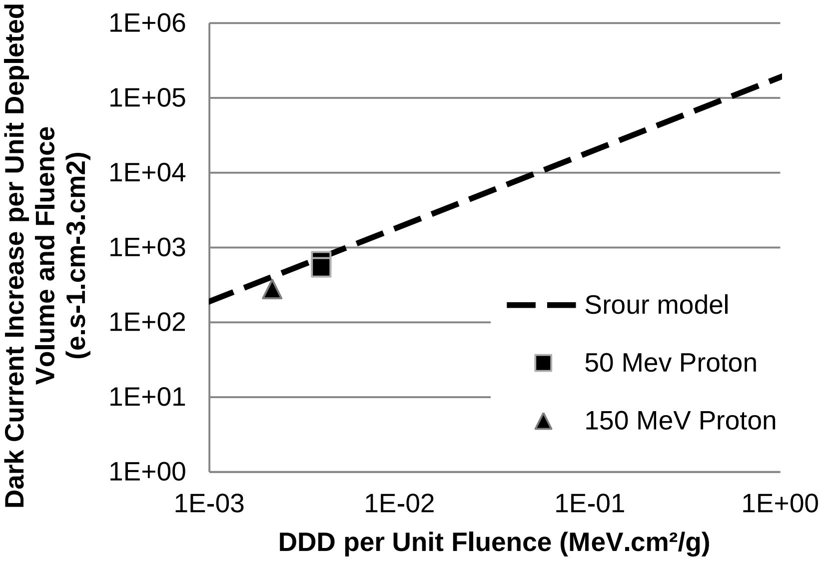

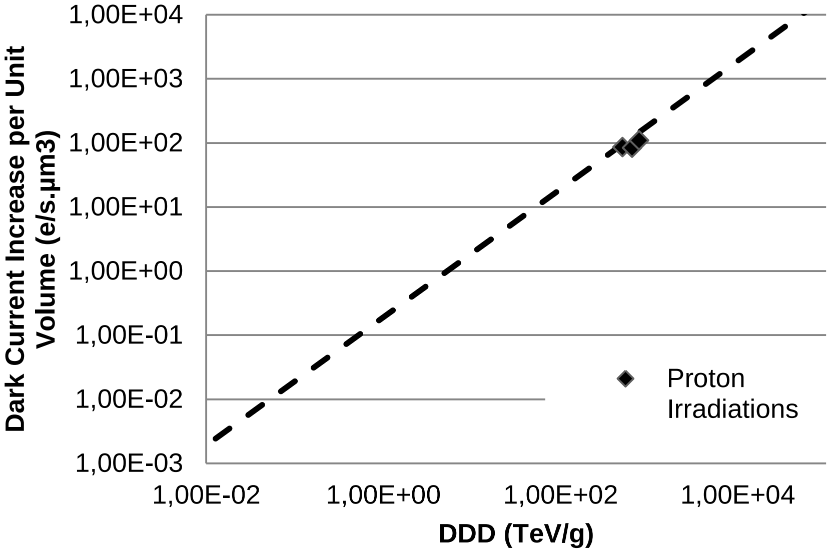

Dark Current Distribution

IRRADIATION PARAMETERS

Sensor Ref	A	B	C	D
Particles	Proton	Proton	Proton	Carbon
Energy (Mev)	50	150	1	10
Fluence (cm-2)	1,30 E+11	3,00 E+11	3.00 E+8	1.00 E+10
DDD (Tev.g-1)	504,4	645	+	++
TID (KradSi)	20,49	21,02	-	-

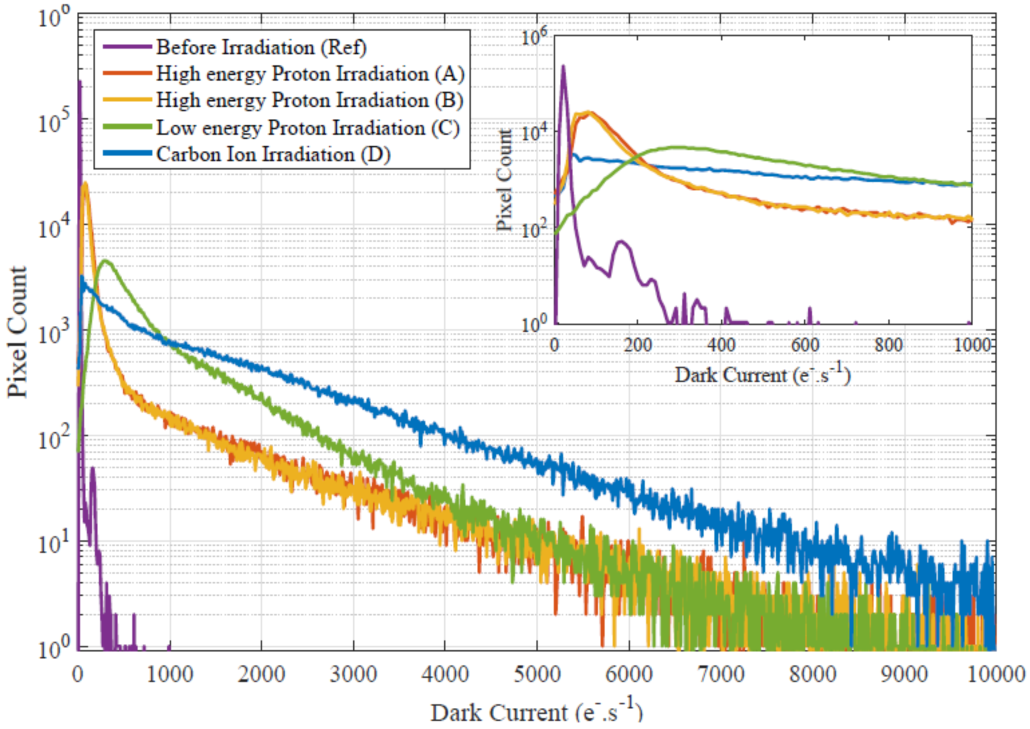

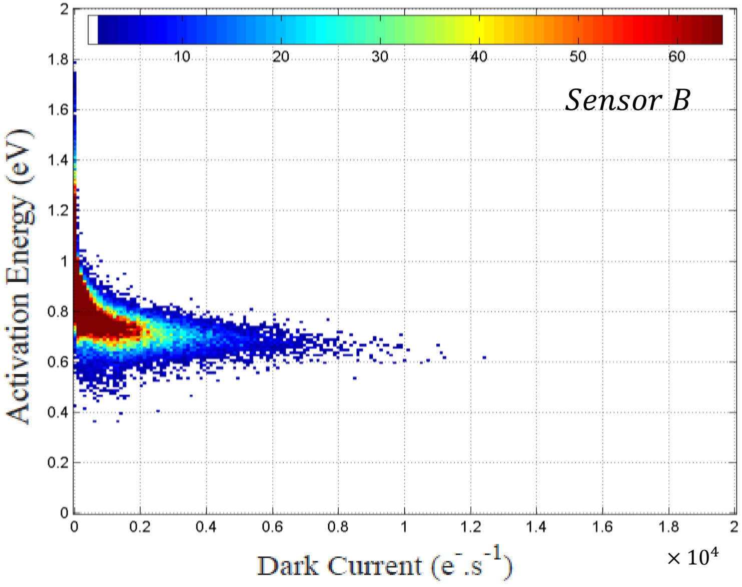

RTS Analysis 1

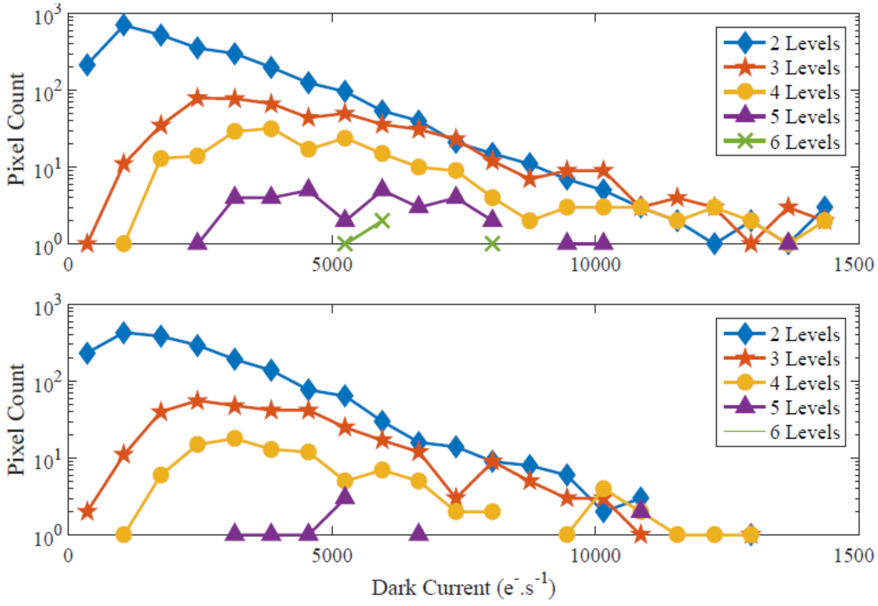

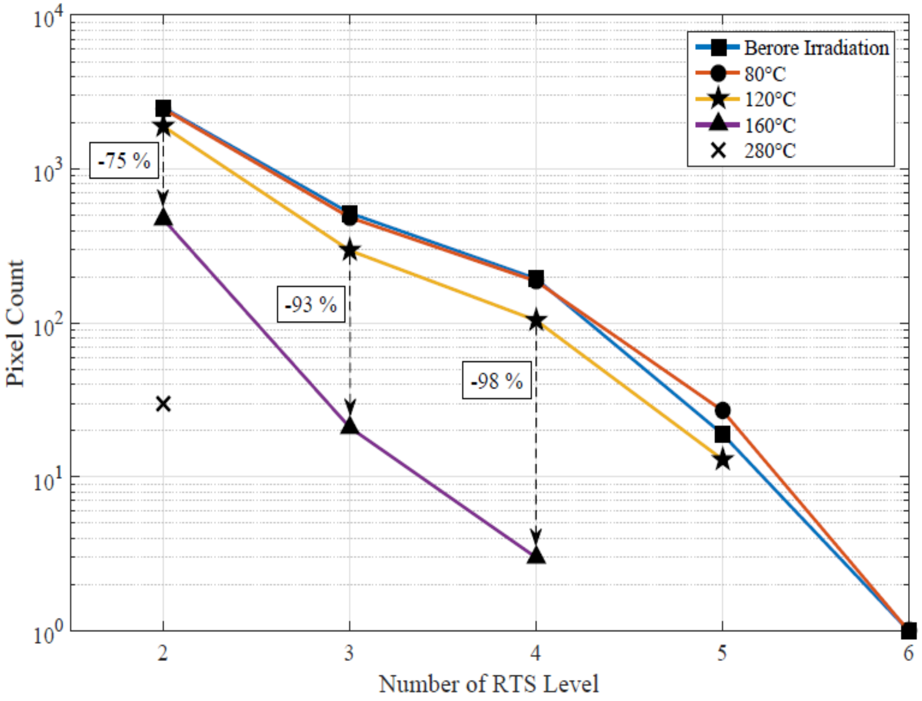

RTS Analysis 2